Ana Cláudia Sardinha Figueiredo

Licenciatura em Engenharia de Micro e Nanotecnologias

Growth of Vanadium Dioxide (VO_2) Nanostructures by Controlling the Hydrothermal Synthesis Parameters

Dissertação para obtenção do Grau de Mestre em Engenharia de Micro e Nanotecnologias

Orientador: Dr. Guy Garry, Research Engineer, TE-OX, Technology Oxides, Paris, France

Co-orientador: Professora Doutora Isabel Maria das Mercês Ferreira, Professora Associada, Faculdade de Ciências e Tecnologia da Universidade Nova de Lisboa, Portugal

Júri:

Presidente: Prof. Doutor Rodrigo Ferrão de Paiva Martins, Professor Catedrático do Departamento de Ciência dos Materiais da Faculdade de Ciências e Tecnologia da Universidade Nova de Lisboa, Portugal

Arguente: Doutora Joana Filipa Quintino Loureiro, Doutorada em Física Tecnológica e Investigadora Pós-doutorada da Faculdade de Ciências e Tecnologia da Universidade Nova de Lisboa, Portugal

Vogais: Prof. Doutora Isabel Maria das Mercês Ferreira Professora Associada, Faculdade de Ciências e Tecnologia da Universidade Nova de Lisboa, Portugal

FACULDADE DE CIÊNCIAS E TECNOLOGIA
UNIVERSIDADE NOVA DE LISBOA

Setembro, 2016

Growth of Vanadium Dioxide (VO_2) Nanostructures by Controlling the Hydrothermal Synthesis Parameters

"If I have seen further it is by standing on the shoulders of Giants."

Isaac Newton

Acknowledgments/Agradecimentos

FRANCE

Pour TE-OX :
L'objectif entier de la vraie éducation n'est pas de rendre les gens capables de faire de bonnes choses, mais de les apprécier ; non seulement laborieux, mais pour profiter du résultat ; non seulement appris, mais à aimer la connaissance ; non seulement pur, mais d'aimer la pureté ; non seulement juste, mais à la faim et soif de la justice. Et j'ai ressenti tout cela depuis le premier jour de mon arrivée en France. Il n'y a pas assez de mots pour remercier les personnes qui ont été avec moi durant cette bataille.

Tout d'abord, je voudrais remercier mon "Best Boss" M. et Dr Guy Garry pour sa gentillesse, son respect, son humour et surtout son courage de m'avoir accepté à TE-OX. J'apprécie encore plus que tout votre esprit ambitieux, vos idées et la résilience de transformer certains projets en réalité. Est-ce possible ? FOR SURE ! Merci beaucoup d'avoir cru en moi. Je ne pourrai jamais oublier la personne que vous êtes. Un grand merci de m'avoir donné cette opportunité qui fût une expérience incroyable.

Oumy, tu as été mon principal soutien durant ces 7 mois. Je ne pourrai jamais oublier ton sourire le premier jour où je suis arrivée. Tu m'as fait comprendre que cette expérience serait une des meilleures expériences dans ma vie avant même que mon projet commence. J'ai compris immédiatement la personne incroyable que tu es. Je ne pourrai jamais oublier tes mots de soutien et tes expressions étonnantes. Tu as fait de moi une meilleure personne, et tu m'as fait comprendre qu'il est possible d'atteindre le bonheur. Nos trajets à St. Quentin, ton rire et tant d'autres choses. Tu donnes vraiment un sens à l'amitié. Tu mérites vraiment le meilleur dans cette vie, et tu l'auras ! Rappelle-toi, que tu seras toujours la bienvenue dans ma maison, car tu es déjà dans mon cœur. Ceci n'est pas un au revoir, car une amitié ne se mesure pas par la distance. Crois en toi comme tu as réussi à me faire croire en moi.

Pour l'ICMMO, Université Paris-Sud :
Mme la Big Boss Corinne Legros, la véritable définition d'une réelle patronne. L'environnement favorable que vous m'avez offert, depuis le début m'a donné le courage de continuer jusqu'au dernier jour de travail. Sans tout cela, cela aurait été impossible. Tous ces moments passés au laboratoire, à la DRX, au bureau, tous ces trajets jusqu'à à la station RER, toutes ces conversations m'ont fait comprendre que dans la vie, il est possible de trouver des personnes extraordinaires qui peuvent nous aider à évoluer beaucoup plus que ce à quoi nous nous attendions.
Céline Byl, votre passion et votre sensibilité pour la science m'ont fait réaliser que vous êtes un des rares exemples vivant qui aime ce qu'il fait. Vos conseils et votre aide m'ont donné une vision différente et meilleure de la science. Vous m'avez montré qu'il est juste nécessaire de croire et de travailler et les choses se produiront. Sans vous, je n'aurais jamais trouvé la meilleure concentration V^{5+}.

Michel Andrieux, je voudrais vous remercier aussi pour votre aide et soutien apportés lors de mon stage. Merci beaucoup pour avoir cru en moi et d'avoir montré un intérêt en mes compétences et capacités. Ces mots m'ont montré que si je veux je peux.

Nathalie Prud'homme, je vous remercie beaucoup pour l'intérêt que vous avez démontré durant tout mon stage, de votre soutien et de compassion. Il était aussi important pour moi d'avoir tant de gens intéressés par mon travail.

M. Patrick Ribot, je ne veux pas vous remercier seulement pour toutes les caractérisations au MEB mais aussi pour votre bonne humeur, votre gentillesse et votre grand sourire que je voyais tous les matins. Merci beaucoup pour la compréhension de mon discours français.

Les derniers mais pas les moindres, Tass, Sébastien, D. Isabel et David, je n'oublierai jamais votre amitié et vos sourires, ils ont fait mes jours et seront toujours dans mon cœur. Un gros bisou pour vous de Miss Ananás.

Chacun d'entre vous possède une signification particulière pour moi, je vous remercie beaucoup pour cette expérience incroyable, et rappelez-vous le talent gagne des jeux, mais le travail d'équipe gagne des championnats.

Andreia, esta é para ti:
Foste uma amiga muito importante nesta grande aventura. O teu apoio, a tua motivação e as tuas maluquices desde o início, foram igualmente fundamentais para me aguentar dentro do desconhecido. Às vezes na vida nem sempre as coisas correm como planeado, todos estes altos e baixos servem para nos fazer adaptar e melhorar. De certeza que melhores tempos virão para todos. Espero que os tempos passados aqui tenham sido igualmente enriquecedores para ti. Desejo o melhor para o futuro, Crazy Girl.

PORTUGAL:

Ao DCM:
Quero deixar um grande obrigado geral a todo o corpo docente do DCM que me acompanhou durante os últimos cinco anos. Obrigada por me terem transmitido todo o vosso conhecimento e pela paciência com todos alunos de Micro e Nano, sem vocês não poderia ser Engenheira.

Quero igualmente agradecer ao Professor Dr. Rodrigo Martins, obrigada por acreditar incondicionalmente nas capacidades dos alunos, por nos disponibilizar a 202 que, no fundo, acabou por ser a nossa segunda casa durante 3 anos e por tentar sempre que dessemos o nosso melhor em tudo o que fizemos e continuamos a fazer.

Sara e Sónia, vocês merecem igualmente um agradecimento, por todo o suporte que oferecem aos alunos sem nunca pestanejar, todo o vosso trabalho é essencial.

Desejo ao DCM o maior sucesso.

À minha orientadora:
Professora Isabel Ferreira, se estou a escrever estes parágrafos é porque desenvolvi um projeto e se desenvolvi um projeto foi graças a si. Todo o suporte incondicional que recebi da sua parte nunca será esquecido. Sem si esta ponte entre Lisboa e Paris não teria sido construída e não teria tido uma experiência emocionante, não teria crescido como cientista e como pessoa. Todos os simples conselhos que me deu desde o início fizeram-me acreditar cada vez mais em mim, acreditei tanto que consegui chegar aqui hoje. Mas quem acreditou mais numa miúda “despassarada” foi a Professora. Um grande, grande obrigado. Nunca a vou esquecer.

Aos meus amigos:
Eu sempre vos disse, ao longo destes anos, que os meus agradecimentos eram para vocês. Não consigo exprimir por palavras o vosso apoio incondicional, a vossa paciência incondicional, mas mais que isso, a vossa amizade incondicional. Sempre disse, um curso não se faz sozinho e vocês são a prova viva disso. O trabalho em equipa, as horas passadas na 202, tudo o que me ensinaram tornou os tempos na Universidade nos melhores momentos da minha vida. Nunca pensei estar tão contente e tão triste de chegar ao fim. Vou ter saudades de tudo um pouco, e de cada bocadinho de vocês, cada um de vós tem um cantinho especial no meu coração. Não foi apenas uma tese, foi todo um percurso académico. A palavra amizade são vocês que a fazem. Se eu fui capaz de ver mais longe é porque estava de pé nos ombros de gigantes. Vocês foram os meus gigantes. Sacanita, Sacanagem, Sacanugem, MINHOS, Bruno Beast a.k.a BB a.k.a Bruno Fernandes, Migu Almeida, Carolinda, Ricardo, Raquel, Primo Rodi, Bibi, Susie Fofi, Sofia (juro que esta ordem foi totalmente aleatória). Quem teria sido eu sem vocês? E quem teriam sido vocês sem mim? Já pensaram nisso?
Especial Agradecimento:
Joana, Constança e Professor João Pedro Oliveira (DE), sem vocês e sem aquele projeto também não seria possível tornar-me Mestre este ano. A vós, um grande obrigado.

Ao Bando dos 4:
A vocês que sempre acreditaram em mim desde o primeiro segundo que pus os pés na FCT-UNL. A vocês que sempre me motivaram para chegar até aqui e a vocês que me foram mostrando que, por

todas as portas que se fecham, existem janelas que se abrem. Não se trata só de uma tese, mas sim de uma grande amizade que quero que seja partilhada com os olhos de quem a lê. A vocês, Padrinho, Gabi e Ana, um enorme obrigado. Beijinhos e até já.

Ao meu amor:
Luís, existem tantas coisas que te quero dizer, meu amor. No meio dessas coisas todas existe tanto amor que bloqueia a escrita da caneta no papel. Há sentimentos, que só demonstrados, há gratidão que só sentida, há amor que só é amor se partilhado. Se estou hoje aqui, sentada nesta cadeira a escrever este texto para ti, foi por ti. Queria tanto, mas tanto conseguir explicar por palavras o que estou a sentir neste momento. És a prova viva de inspiração e motivação. Sentido e orientação, são desvanecidos sem ti, Luís. Vou sempre lutar por ti e por nós até à exaustão, até não te conseguir mais provar o quão és importante para mim e o quão contribuíste para os momentos mais importantes na minha vida. Ainda bem que não entrei na Universidade no momento em que devia, ainda bem que foi Micro e Nano, ainda bem que foste tu. E se perguntarem, o que é que Micro e Nano te ofereceu? Eu vou responder, sem hesitar, ofereceu-me o meu amor da minha vida. Era suposto? Sem dúvida!

À Família Ferreira:
Família Ferreira, quero-vos deixar um especial agradecimento do fundo do meu coração, por me tratarem desde sempre como um membro da família, por me incluírem em todos os vossos projetos e planos, por me fazerem sentir especial entre vós. Todo o carinho e apoio por vocês demonstrado foi sem dúvida igualmente crucial para chegar hoje aqui. Sei que no fundo sempre acreditaram que era capaz. Nunca vou esquecer, vão estar sempre no meu coração. Filipe Vitória, isto também se aplica a ti.

E por último, e mais importante, aos meus Pais e à minha Irmã:
Mãe Lina, Pai Jorge e Mana Catarina, sempre lutei até ao limite o mais que consegui para vos deixar o mais orgulhosos possível de mim. Todo o esforço que pus neste percurso académico foi por vocês. O meu objetivo não foi só acabar o que comecei, mas também vos provar que sem esforço não há progresso, quero-vos fazer sentir que fui a prova viva disso. Espero que tenha conseguido, no fundo eu sei que sim. O amor incondicional entre nós é a minha motivação e será sempre para alcançar o sucesso. Penso que nunca vos vou conseguir compensar por tudo o que me deram até hoje, pela vossa educação e, mais importante, por me terem sempre deixado tomar as minhas decisões. Vocês não são só os meus pais, são os meus melhores amigos. Nunca vos vou deixar sós, podem confiar na minha palavra. Catarina agora é a tua vez! Força, vais conseguir, não duvido nem por um segundo! O meu orgulho é também o vosso! Este percurso académico também é vosso, no fundo, é de todos nós.

Abstract

Vanadium dioxide (VO_2) has been intensively studied as it undergoes a metal-insulator phase transition (MIT) and exhibits numerous polymorphs. Therefore, it is very promising for MIT-based electronic and optoelectronic devices. The control of VO_2 growth to obtain 1D micro and nanostructures has recently attracted more interest and opened doors for new optoelectronic applications. Herein, pure phase of VO_2(B) and VO_2(A) nanostructures have been synthesized by hydrothermal treatment in V_2O_5-$H_2C_2O_4$-H_2O system. The hydrothermal synthesis conditions were studied in order to observe the formation and evolution of VO_2(B) and VO_2(A) phases. Experiments showed that VO_2(B) phase was firstly formed and then transformed into VO_2(A) with the increase of hydrothermal reaction time from 8h to 72h. Additionally, it was studied the influence of some modifications on the hydrothermal synthesis process. The composition and morphology of the as-obtained samples were characterized using X-ray diffraction (XRD), Scanning electron microscopy (SEM), Fourier transform infrared spectroscopy (FTIR) and Raman spectroscopy. Furthermore, the phase of transition temperatures and oxidation resistance of the as-obtained samples were evaluated by differential scanning calorimetry (DSC). In addition, the present study also provides an indirect way to obtain VO_2(M), more precisely by calcination and laser annealing of VO_2(B) and VO_2(A), respectively.

Keywords: Vanadium dioxide, polymorphs, metal-insulator phase transition, hydrothermal synthesis.

Résumé

Le dioxyde de vanadium (VO_2) est un exemple de matériau qui a été étudié de manière intensive car il présente une transition de phase métal-isolant (MIT). Le VO_2 présente un diagramme de phases varié avec de nombreux polymorphes ; il est considéré comme étant le matériau d'avenir des futurs dispositifs électroniques et optoélectroniques à base de MIT. Depuis quelques années, il y a un intérêt croissant dans le contrôle des micro- et nanostructures de VO_2 pour le comportement 1D de leurs propriétés physiques mais aussi pour des applications comme des capteurs. Dans cette étude, des nanostructures de phases pures VO_2(B) et de VO_2(A) ont été synthétisés par traitement hydrothermal à partir d'une solution contenant du V_2O_5-$H_2C_2O_4$-H_2O. Huit séries d'échantillons ont été préparées en faisant varier les conditions de synthèse hydrothermale afin d'observer la formation et l'évolution des phases de VO_2(B) et de VO_2(A). Les expériences ont montré que la phase VO_2(B) est d'abord formée puis se transforme en VO_2(A) lorsque que le temps de réaction de la synthèse hydrothermale passe de 8h à 72h. Des expériences supplémentaires ont été réalisées afin d'étudier l'influence de certains facteurs extrinsèques sur la formation des nanostructures de VO_2. La composition et la morphologie des échantillons obtenus ont été caractérisées respectivement par diffraction des rayons X (DRX), par microscopie électronique à balayage (MEB), par spectroscopie infrarouge à transformée de Fourier (FTIR) et par spectroscopie Raman. De plus, la calorimétrie différentielle à balayage (DSC) a été utilisée pour déterminer la température de transition de phases et de résistance à l'oxydation des échantillons. Finalement, la présente étude montre une manière indirecte d'obtenir du VO_2(M) par calcination et par recuit laser du VO_2(B) ou du VO_2(A).

Mots clés : Dioxyde de vanadium, polymorphes, transition de phase métal-isolant, synthèse hydrothermale.

Resumo

O dióxido de vanádio (VO_2) é um material que tem atraído os investigadores devido à particularidade de apresentar uma transição de fase entre metal e isolante a uma temperatura definida que depende da sua composição e das fases cristalinas obtidas após síntese. Assim, é um material que promete novos desenvolvimentos de dispositivos eletrónicos e optoelectrónicos baseados na transição metal-isolante (MIT). O controlo do crescimento de micro e nanoestruturas 1D de VO_2 tem vindo a aumentar e a abrir portas para a criação de novas aplicações. Na presente dissertação, a fase pura de nanoestruturas de VO_2(B) e VO_2(A) foram sintetizadas pela técnica hidrotermal através de um sistema V_2O_5-$H_2C_2O_4$-H_2O. Foi estudada a influência dos parâmetros da técnica hidrotermal na formação e evolução das fases VO_2(B) e VO_2(A). Os resultados obtidos mostram que a fase (B) é primeiramente formada e, em seguida, transformada em fase (A), com o aumento do tempo de reação de 8h para 72h. Foram realizadas experiências adicionais de modo a estudar a influência de modificações ao processo de síntese na formação de nanoestruturas de VO_2. A composição e a morfologia das amostras obtidas foram caracterizadas através de difração de raios-X (DRX), microscopia eletrónica de varrimento (SEM), espectroscopia de infravermelho com transformada de Fourier (FTIR) e espectroscopia de Raman. Além destas caracterizações, a transição de fase por aumento de temperatura e a resistência à oxidação das amostras obtidas foram também avaliadas por calorimetria de varrimento diferencial (DSC). O presente estudo descreve ainda, uma forma indireta de obter VO_2(M) por calcinação e recozimento por laser de VO_2(B) e VO_2(A), respetivamente, obtidas previamente através da técnica hidrotermal.

Palavras-chave: Dióxido de vanádio, nano-cristais, transição metal-isolante, técnica hidrotermal.

Table of Contents

List of Figures

List of Tables

Abbreviations

1D	One dimensional
A200	200 ml Teflon-lined autoclave
A300	300 ml Teflon-lined autoclave
ATR-FTIR	Attenuated Total Reflection - Fourier Transform Infrared Spectroscopy
CVD	Chemical Vapor Deposition
DSC	Differential Scanning Calorimetry
DTA	Differential Thermal Analysis
FTIR	Fourier Transform Infrared Spectroscopy
HTP	High Temperature Phase
HT-XRD	High Temperature-X-Ray Diffraction
ID	Identification
IR	Infrared
JCPDS	Joint Committee on Powder Diffraction and Standards
LTP	Low Temperature Phase
MIT	Metal-Insulator Transition
MOTTFET	Mott-Field Effect Transistor
ODA	Octadecylamine
PVD	Physical Vapor Deposition
SEM	Scanning Electron Microscope/Microscopy
SEM-FEG	Scanning Electron Microscope-Field Emission Gun
Si	Silicon
TEM	Transmission Electron Microscopy
XPS	X-Ray Photoelectron Microscopy
XRD	X-Ray Diffraction

Symbols

O/O_2	Oxygen
V	Vanadium
VO	Vanadium oxide/monoxide
VO_2	Vanadium dioxide
V_6O_{13}	Hexavanadium tridecaoxide
V_4O_9	Tetravanadium nonaoxide
V_3O_7	Trivanadium heptaoxide
V_2O_5	(Di)vanadium pentoxide
V^{5+}	Vanadium (V) oxide (V_2O_5 ion)
V^{4+}	Vanadium (IV) oxide (VO_2 ion)
W	Tungsten
Mo	Molybdenum
F	Fluorine
H_2	Hydrogen
H_2O	Water
$H_2C_2O_4$	Oxalic acid
H_2SO_4	Sulfuric Acid
CH_3CH_2OH	Ethanol
$V_3O_7.H_2O$	Trivanadium heptaoxide hydrate
Ar	Argon
C	Carbon
CO_2	Carbon dioxide
pH	Potential of hydrogen
M	Molar
Mw	Molecular weight
g	Gram
mol	Mol
L	Liter (SI) – mL, µL
m	Meter (SI) – cm, mm, µm
Å	Angström
A	Ampere (SI) – mA
V	Volt (SI) – kV, mV
W	Watt (SI) - mW
K	Kelvin
ºC	Degrees Celsius
J	Joules
Pa	Pascal
h	Hour
s, sec	Seconds
min	Minutes
%	Percentage
λ	Wavelength
rpm	Revolutions per minute
º	Degree
θ	Theta
T	Temperature
$[V^{5+}]$	Concentration of V^{5+} in solution
t	Time
f	Filling percentage
Tl	Teflon liner
Tc	Critical temperature
a, b, c	Lattice parameters

Objectives

The main purpose of this work is to synthesize quasi-spherical VO_2(M) nanostructures with uniform size (200-300 nm width and above 500 nm length) by controlling the hydrothermal synthesis parameters, in particular the synthesis temperature, the V^{5+} concentration in solution, the synthesis time and filling percentage, keeping other conditions constant. The growth of such nanostructures will allow the perception of the effect that each synthesis parameter has on the formation of different VO_2 phases, shapes and sizes. For this type of synthesis route, the conditions used to carry the reactions are very dependent on other factors, such as the volume of the autoclave used to carry the reaction. So, the first challenge is to achieve a pure phase of VO_2(B), which is always formed firstly, and then refine and adapt the parameters in order to observe its evolution into VO_2(A), and further into VO_2(M).

Regarding VO_2 properties, this work takes phase transitions and morphology control through hydrothermal synthesis as inspiration to construct, in a near future, some promising devices such as the MOTTFET.

VO_2(M) particles present snowflake aggregation with preferential orientation growth along the (110) direction, limiting their dispersion and overall application to micro and nanodevices. Thus, in an attempt to achieve the best VO_2(M) morphology and size, the influence of additional modifications on the hydrothermal synthesis process were also appraised: the influence of Teflon liner, autoclave's volume, non-stirring and the presence of a Si substrate. Finally, after carrying a continuous process of VO_2 synthesis, the crystallinity of these samples and the phase transitions through other routes than hydrothermal synthesis will be evaluated.

1. Introduction

1.1. Metal-Oxide Nanostructures

One dimensional (1D) nanostructures of metal-oxides have received great attention from researchers, not just due to their mixed valence compositions and active surface area, but also because they often exhibit specific optical, electrical, physical and chemical properties, which are significantly different from their bulk materials [1]–[5].

Many nanoscale materials, such as nanotubes, nanorods, nanofibers, short belt-like nanoparticles and nanowires, have been described during the past few years and they are now accessible in several material systems with well-developed morphology [3], [6]. Mastery over the morphology of nanomaterials enables control over their properties, which is also quite useful to apply them in nanodevices [4], [5].

Despite the significant progress over the last few decades, shape-controlled synthesis of micro and nanostructures remains a challenge [5]. Therefore, many syntheses are being explored and developed, more precisely to control the morphology, shape, size and crystalline structure of the 1D metal-oxide nanostructures, especially the 1D vanadium dioxide (VO_2) nanostructures, which have raised considerable attention due to their unique chemical (such as electrochemical [4], physical and special optical properties [7]) which make them highly desired in a wide range of promising potential applications [4], [7].

1.2. VO_2 – Structure and Applications

Vanadium presents a large variety of oxidation states (+3 to +5), forming several binary oxides (like VO, VO_2, V_6O_{13}, V_4O_9, V_3O_7, or V_2O_5, among others) with exceptional chemical, structural and optoelectronic properties [8]–[10]. Due to that fact, vanadium based oxides and their related compounds have been widely studied for electronic and optoelectronic device applications [10]–[13]. From all vanadium oxides, VO_2 has been the most studied due to a variety of polymorphism leading to phase transition at relatively low temperature [10], [11], [14], enabling metal-insulator transition (MIT), which is specially suitable for memory electronic devices. So far, more than ten kinds of polymorphic forms of V-O system have been reported, mainly including monoclinic VO_2(B) (C2/m space group), tetragonal VO_2(A) ($P4_2$/nmc space group), tetragonal rutile-type VO_2(R) ($P4_2$/mnm space group) and monoclinic rutile type VO_2(M) ($P2_1$/c space group) [3], [10], [12], [15]. Their crystal structures are presented in **Figure 1.1** and their crystallography data, as well as their traditional morphology along with observations, can be consulted in **Appendix 1**-**Table A1.1 and Figure A1.2 and A1.3**, respectively**.** In particular, the rutile type VO_2(R), which is considered as the most stable structure for VO_2, and the monoclinic VO_2(M), which exhibits a very fast and reversible metal-insulator transition at low temperature, are the ones requiring more attention [3], [15], [16]. Other metastable phases of VO_2, mainly VO_2(B) and VO_2(A), are also of great interest due to their promising properties at nanoscale [3], [11]. Even though VO_2 has been widely studied, it still remains quite a challenge to fully understand how the preparation conditions control their polymorphism [3], [17].

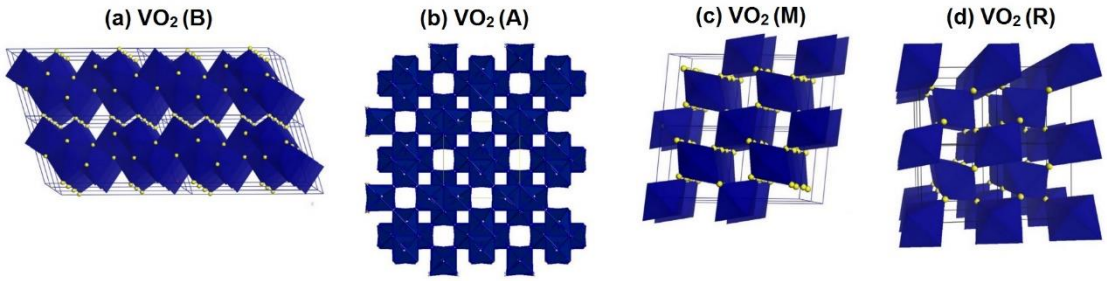

Figure 1.1. Crystalline structure of (a) VO_2(B), (b) VO_2(A), (c) VO_2(M) and (d) VO_2(R) phases [18].

1.2.1. Metal-Insulator Transition (MIT) in VO_2

MIT, in which a high-temperature metallic state is transformed into a low-temperature insulating state at a critical temperature (*Tc*) [18], is also named Mott-MIT phenomena, more precisely due to its similarity with purely electronic Mott transition of a metal to a Mott-Hubbard insulator driven by Coulomb repulsions and a charge-density wave transition. MIT debates not only about the electron-electron correlation effect but also about the electron-lattice interaction, which is referred to as Peierls MIT, arising from a lattice structural change in a material and consequently inducing a lattice deformation [18], [19]. An electronic MIT and a structural transition often occur simultaneously [18].

The MIT of VO_2 in the rutile and monoclinic (R and M) families of compounds has been extensively studied due to its importance for several technological applications [18]. VO_2 is transformed from an insulating state to a metallic state at about 68 ºC (*Tc*), which is usually accompanied by a crystallographic transition between a low temperature monoclinic phase (M) and a high temperature tetragonal phase (R) (**Figure 1.2**) [10]. This transition is reversible and it causes not just an abrupt change of the VO_2 electric and magnetic properties but also a sharp variation of its optical transmittance [13], [14]. MIT in VO_2 can be induced by several factors, such as thermal heating, magnetic field, electrical and optical excitations, structural stress, among others [20], [21]. Although *Tc* of VO_2 is already interesting for several electronic applications, the lowering of *Tc* towards room temperature will enlarged the field of application of this material. Thus, several studies have demonstrated that *Tc* can be reduced by elemental doping (with W-Tungsten, Mo-Molybdenum, F-Fluorine etc.). However, doping will decrease the magnitude of the MIT, promoting even more changes in electric and optical properties. The *Tc* can also be modified with strain, grain size, non-stoichiometry or a combination of the above factors [10], [15]. Moreover, it is very meaningful for material scientists to study MIT and its possibility to occur on an ultrafast time scale, since it may have some prominent applications.

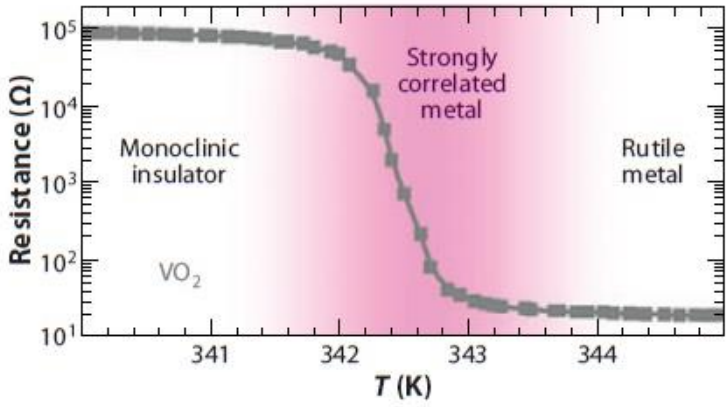

Figure 1.2. Thermal triggering of MIT in VO_2 [20].

1.2.2. State of the Art: Applications of VO_2

The combination of the VO_2 ideal functional properties opens up several opportunities for many promising applications in different fields of expertise. In fact, this material has been widely investigated as a potential candidate for the cathode in lithium-ion batteries for electric and hybrid vehicles [14], [22]. The transition phase properties of the VO_2 makes its related compounds to be suitable for new types of ultrafast electrical and optical devices: optical and electrical data storage mediums, optical modulators, thermal and chemical sensors, optical switching, memresistive elements, thermochromics, smart windows coatings to block solar infrared radiation above a certain temperature, and so on [8], [14], [16], [20]. The illumination of materials with the same properties as VO_2, with intense light beams, can produce heat and induce modifications in the crystal structure [8]. Once more, the MIT in VO_2 is in foreground and it can also be exploited in microwave electromagnetic switches, more precisely for the reconfiguration of communication networks, radar components and microwave complex circuits, such as antenna arrays [23], [24]. Many more potential applications based on its transition phase properties may be found in the future [3].

Among the crystalline phases of VO_2, VO_2(M) presents a good thermal stability and oxidation resistance, which makes such compound suitable for several applications in the air [25].

Mainly due to Mott insulator effect, nanostructured vanadium oxide also could be used in many other fundamental researches, in particular Mott-field effect transistor (MOTTFET), which is one of the most promising applications. The MOTTFET, several times reported by the inventor and scientist Stanford R. Ovshinksky earlier on 1940s on his researches, actually represents the next generation of electronic devices, since it faces the challenge of adding new functionalities to classic devices, such as transistors, more specifically by integrating nanostructures that undergo through phase transitions [26], [27]. Thus, many research studies are being made in order to identify the potencial of VO_2 in overcoming the limits of Si transistors [28].

One of the main goals for a real development of VO_2 nanostructures consists in fully understanding not only their formation and morphology but also their intrinsic properties, in order to be able to build specific and personalized devices. The control of the transitions phase temperature and speed are some of the

highest priority tasks because the functionality of VO_2 and its potential scope of application strongly depend on these two parameters [29].

1.3. Methods to Synthetize VO_2 Nanostructures

So far, various techniques have been developed for the preparation of VO_2 nanostructures in the form of thin films or nanoparticles [22]. VO_2 nanostructured thin films can be prepared by several methods, such as atomic layer deposition, ion beam deposition, sputtering deposition techniques, electron beam evaporation, physical/chemical vapor deposition (PVD/CVD), pulsed laser, sol–gel and so on [13]–[16], [21], [30]. However, most of these techniques are usually very complex, presenting a low efficiency and a high cost [10]. In addition, crystalline nanoparticles can be superior to thin films, since they have the advantage to be made in a single domain, allowing a lower concentration of defects [31]. VO_2 nanostructures in the form of nanoparticles can be prepared by many methods, such as pyrolysis of precursor powders, spray pyrolysis, thermal treatment, sol–gel and hydrothermal reaction [10], [15]. Hydrothermal method has been considered the main route to synthesize VO_2 nanoparticles due to its uncomplicated process (it does not need rigid experimental conditions or special equipment), low cost, large-scale and mass productivity [10].

1.3.1. Preparing Nanostructures of VO_2 via Hydrothermal Synthesis

Hydrothermal synthesis has been considered as the main route to obtain nanostructured VO_2 in the form of single particles. This technique is defined as a crystal growth under conditions of high temperature and pressure, more specifically by using water as a reaction medium in a closed system [32]. The most common temperatures used vary within the range between 100-374 ºC (critical temperature of water). In this particular temperature range, the pressure varies in the exponential function and up to 250 bar. It is established, and inside the autoclave, a vapor-liquid equilibrium, which provides an autogenous pressure. Under these conditions, water has a dissolving power greater than the atmospheric pressure. Hydrothermal route offers not just the previously reported advantages but also a good control on morphology, final products with high crystallinity, chemical stoichiometry and the opportunity to explore new phases [32]–[35]. All these benefits result from the possibility to set and change the hydrothermal synthesis conditions, such as: precursor materials, synthesis time, temperature, concentration, filling percentage of the autoclave, pressure, pH etc. [12]. However, such method also presents some advantages, namely: a high pressure may cause accidental explosions and it is required a prior knowledge on solubility of precursor materials [35].

The most suitable way to grow VO_2 nanostructures, and under hydrothermal conditions, is through a Teflon-lined autoclave, which is capable of sustaining a highly corrosive solvent at a high temperature and pressure for a long period of time [36]. Inside the autoclave, a synthesis takes place, which is based on the reduction of vanadium oxides precursors (reduction of V^{5+} in V^{4+}). Different reducing agents, such as organic acids, can be used under the desired work conditions to achieve good quality products. However, most of the authors choose the vanadium pentoxide (V_2O_5) as precursor and the oxalic acid ($H_2C_2O_4$) as reducing agent as the model system to describe nanostructured materials [6], [11], [14], [15], [22], [37]–[39]. In addition, in a typical procedure the authors use the appropriate amount of V_2O_5

and $H_2C_2O_4$ (1:(1-3) in molar ratio) and directly add to an appropriate volume of deionized water, considering that the reduction is completed when a clear transparent dark blue solution is formed [3], [14], [22], [38].

1.3.2. Influence of the Hydrothermal Synthesis Parameters

Some authors have revealed that the pure phases of VO_2(B), VO_2(A) and VO_2(M), as well as their transformation, can be controlled in this system through the variation of the previously described parameters. H.F.Xu et al. [11], Shidong Ji et al.[3] and Srinivasa R.P et al. [37] have reported the formation of VO_2(A) through hydrothermal treatments carried out at temperature ranges from 180 ºC to 230 ºC for different periods of time (12h to 48h). The conclusions have shown that more than 24h, and at least 230 ºC, are necessary to transform VO_2(B) in VO_2(A) phase. Zang et al. [40] have also obtained VO_2(A) nanostructures from two hydrothermal processes, more precisely by treating an already hydrothermally prepared VO_2(B) sample at 280 ºC for 48h. In addition, Shidong Ji et al. [14] also showed the importance of the filling percentage in the hydrothermal route. They conclude that, when the synthesis conditions (temperature and time) remain the same, and if the filling percentage increases from 40% to 60%, VO_2(A) is transformed into VO_2(M). The authors also showed that more than 24h and a high temperature (from 260 ºC to 270 ºC) are required to transform VO_2(A) into VO_2(M) phase.
Shidong Ji et al. [22] do not simply show the influence of the time and temperature on the hydrothermal process but also the influence of pH. They adjust this parameter (3.5 to 1.8) with sulfuric acid (0.5 M), concluding that it has an important role in the morphology of the obtained crystals. Hong-Yi Li et al. [4] used octadecylamine (ODA) as a reducing agent and structure directing template during the hydrothermal process of VO_2 nanostructures. Authors have found that the morphology of the final products can be tuned by the reaction of the pH, more precisely due to its influence on the form of vanadium precursor, and by the ODA concentration due to the rolling force resulting from hydrophobic clustering of ODA molecules. In spite of the information and studies reported, the influence of the synthesis parameters may change depending on the autoclave's volume.

1.3.3. Alternative Routes for Phase Conversions in VO_2

Additional routes using hydrothermally prepared VO_2 nanostructures for phase conversions are being explored: Yifu Zhang et al. [25] transform hydrothermally prepared VO_2(B) nanostructures into VO_2(M) phase by heating treatment. In addition, it is also very common to use laser heating monitored by Raman spectroscopy to trigger the phase transition of VO_2 nanostructures [8], [41]. It is believed that the study of the hydrothermal treatment parameters on the formation of VO_2 nanostructures provides not just an effective way to control the desired VO_2 phase but also helps to understand all their intrinsic properties.

2. Experimental Section

2.1. Materials

Specifications of the autoclaves can be consulted in **Appendix 2-Tables A2.1 and A2.2**.
Autoclave Maxitech France: stainless steel body (200 ml and 300 ml in capacity), Teflon liners (140 ml and 233 ml in volume capacity), process temperature regulator (Invensys Eurotherm 3208), temperature safety regulator (Invensys Eurotherm 3216), oven, metallic support.
V_2O_5 powder (Mw = 181.88 g/mol, assay > 99.6%, Sigma-Aldrich), $H_2C_2O_4$ solid powder (Mw = 90.03 g/mol, assay = 99.0%, Sigma-Aldrich), deionized water (H_2O) (Mw = 18.02 g/mol), absolute ethanol (CH_3CH_2OH) (Mw = 46.07 g/mol, assay = 99.5%, TechniSolv).
Silicon substrate orientated <100> (10 × 10 mm^2, 0.7 mm thick, International Wafer Service).
Current lab equipment, such as pH paper meter, precision scale (Sartorius), oven (Memmert), tube furnace (Adamel, type: T5HT), hotplate stirrer (Heidolph, MR Hei-Standard) and centrifuge (2-5, Sigma).

2.2. Hydrothermal Method

The synthesis of VO_2 nanostructures was carried out by the hydrothermal method at a moderate temperature and under autogenous pressure. The autoclave design used to synthesize VO_2 samples was the Autoclave Maxitech France, composed mainly by two different stainless steel bodies (200 ml and 300 ml in volume capacity, respectively), two Teflon liners (140 ml and 233 ml in volume capacity), an oven with the respective support and two temperature controllers (**Appendix 2 – Figure A2.1**).
These autoclaves can be heated up to 250 ^oC and under 234 bar. Due to the large thermal expansion coefficient of Teflon liner versus metal (the material in which the liner is enclosed), the Teflon will expand and contract much more upon heating and cooling cycles than its enclosure material. Therefore, a closure mechanism must be used to maintain a constant pressure on the Teflon seal, during both heating and cooling cycles.
The autoclave was installed on a hotplate stirrer (at 300 ^oC, 1400 rpm). The heating of the autoclave was achieved with a coiled heating oven around its outer walls. The oven was connected to a temperature regulator (Invensys Eurotherm 3208), which allows setting up and controlling the external temperature of the system. A thermocouple, secured on the inner walls of the autoclave, was connected to a temperature safety regulator (Invensys Eurotherm 3216) that displays the temperature inside the autoclave (synthesis temperature). The complete setup can be consulted in **Appendix 2- Figure A2.2**.
During all the experiments, the synthesis temperature was imposed by the external temperature with a heating rate of 4^oC/min.

2.2.1. Preliminary Test of the Autoclave

The autoclave was firstly tested with pure water and prior to the heating process. The amount of water used in this pre-treatment did not exceed 40% of the capacity of the cup. The filling percentage of the autoclave has a direct influence on the pressure that is auto-generated inside the autoclave during the synthesis. The pressure formed during the synthesis was subjected to a first approximation to the ideal gas law (**Equation 1**)[42]:

Equation 1

$$PV = nRT$$

where, P is the pressure of the gas (Pa), V is the volume occupied by the gas (m^3), n is the amount of substance of gas (mol), R is the ideal, or universal, gas constant (8.314 $J \cdot K^{1} \cdot mol^{-1}$) and T is the temperature of the gas (K). However, it is not possible to calculate the exact pressure inside the autoclave, since the amount of the solution that is obtained in the vapor phase is unknown.

2.2.2. Preparing VO_2 Solutions

Solutions were prepared based on the results reported in literature [11], [14], [15], [22], [37].
All of the chemical reagents used in the experiments were of analytical grade and without any further purification. In a typical procedure to prepare VO_2 samples, the appropriate amount of V_2O_5 and $H_2C_2O_4$ solid powder (1:(1-3) in molar ratio) was directly added to the appropriate volume of deionized water at room temperature. The orange suspension was continuously stirred at 1000 rpm until a clear transparent dark blue solution (pH=3) was formed (**Figure 2.1**).

Figure 2.1. Evolution of the solution color (during the reduction of V^{5+} (orange) in V^{4+} (dark blue).

All the appropriate quantities, which were previously referred, are dependent on the *input* data (V^{5+} concentration in solution, volume of the autoclave and its respective filling percentage). **Table 2.2.1** shows the amounts used to prepare VO_2 solutions, considering the *input* values.

Referring to the results achieved below, at an early stage and based on previous works, a solution with a V^{5+} concentration of 0.0268 mol/l was prepared. This first choice directed the final solution to a green color, implying that V^{5+} was not completely reduced into V^{4+}. Therefore, it was decided to increase the first chosen concentration until a dark blue color was achieved. Several tests with different concentrations and V_2O_5:$H_2C_2O_4$ in molar ratio (1:1; 1:2; 1:3) were performed, being possible to conclude that the molar ratio must be 1:3 and the V^{5+} concentration at least twice the first value chosen, in order to obtain a pre-reduction.

Table 2.2.1. Prepared solutions of VO_2 for hydrothermal synthesis, identification and amounts of V_2O_5, $H_2C_2O_4$ and H_2O used, considering the *input* values.

***Input* values**			**Quantities**		
V^{5+} (mol/l)	**Autoclave's Volume (ml)**	**Filling (%) of the steel body**	**V_2O_5 (g)**	**$H_2C_2O_4$ (g)**	**H_2O (ml)**
0.0268	200	30	0.1462	0.2172	60
0.0486	200	30	0.2649	0.3934	60
0.0971	200	30	0.5298	0.7868	60
0.1460	200	30	0.7947	1.1802	60
0.0971	300	30	0.7947	1.1802	90
0.0971	300	60	1.5894	2.3604	180
0.1460	300	30	1.1921	1.7703	90

2.2.3. Hydrothermal Synthesis Conditions

During the development of this work, the influence of several hydrothermal synthesis parameters on the preparation of crystalline VO_2 polymorphs was evaluated, in particular the synthesis temperature, the V^{5+} concentration in solution, the synthesis time and the filling percentage of the Teflon liner/steel body, while other synthesis conditions were kept constant in all experiments. In a typical procedure, the appropriate volume of VO_2 samples was transferred into a Teflon-lined autoclave with stainless steel body (200 ml in capacity), followed by hydrothermal treatment under auto-generated pressure at different temperatures for different periods. The thermocouple was placed inside the autoclave during all the syntheses and in the same position (**Appendix 2-Figure A2.3),** in order to measure the synthesis temperature in the same conditions.

After hydrothermal treatment, the autoclave was naturally cooled down to room temperature. The resulting precipitates were collected and washed several times by centrifugation, more precisely with deionized water and absolute ethanol at 2500 rpm for 30 min, and finally dried in an oven at 80 ºC for 15 min. The collecting process of such samples was based on the results reported in literature [11], [14], [15], [22], [33], [37]. **Figure 2.2** shows the complete synthesized VO_2 nanoparticles colleting process.

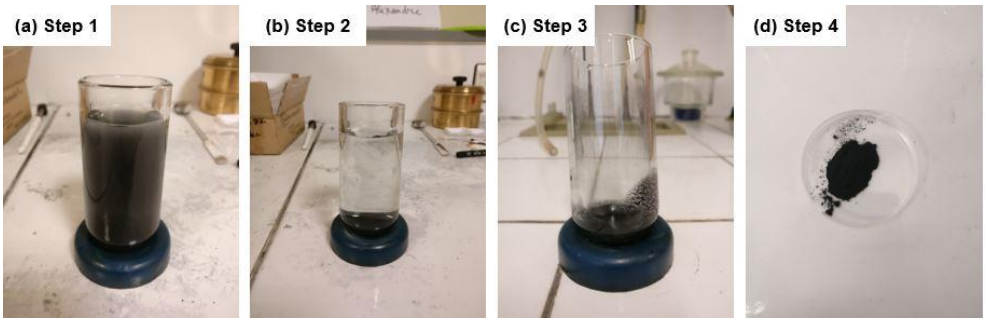

Figure 2.2. Synthesized VO_2 nanoparticles colleting process.
(a) Step 1: black solution of VO_2 nanoparticles extracted from the autoclave after hydrothermal synthesis and before centrifugation; (b) Step 2: suspension of VO_2 nanoparticles after centrifugation with absolute ethanol at 2500 rpm during 30 min; (c) Step 3: VO_2 nanoparticles after removing the ethanol; (d) Step 4: VO_2 nanoparticles after drying in an oven at 80°C during 15 min resulted in a black powder.

In order to confirm if the influence of the hydrothermal parameters on the final VO_2 nanostructures may change depending on autoclave's volume used, hydrothermal syntheses that followed the same procedure previously described were performed to evaluate the structure and morphology of the as-obtained products. When the autoclave's volume has changed from 200 ml to 300 ml, the synthesis parameters have kept the same. In addition, it is important to refer that during the synthesis process the Teflon liner fitting the 200 ml steel body autoclave, has melted due to the high temperature inside, therefore some final tests were performed through the 300 ml Teflon lined autoclave.

In addition, supplementary tests that monitored the same process were done, with the aim to study the influence of the hydrothermal synthesis parameters when these are taken to the extreme, the Teflon liner absence during the hydrothermal synthesis as well as the effect of non-stirring on the VO_2 final structure. Moreover, an additional test has been carried out in order to evaluate if it was possible to grow VO_2 nanostructures in specific directions, namely in <100> direction. For this purpose, a Silicon substrate orientated <100> (10 x 10 mm^2) (**Appendix 3-Figure A3.1**) was placed at the bottom of the 300 ml Teflon-lined autoclave and a hydrothermal synthesis was performed at 238 ºC for 8h, with a V^{5+} concentration of 0.0971 mol/l and a filling percentage of 30%, without stirring.

Hydrothermal synthesis conditions used to perform the additional experiments are described in **Appendix 4.** Most relevant hydrothermal synthesis conditions used to obtain VO_2 nanostructures are shown in **Table 2.2.2.** All the experimental details and respective results can be found in **Appendix 5-Table A5.1**.

Table 2.2.2. Hydrothermal synthesis parameters used in the production of VO_2 nanostructures, through a steel body of 200 ml and 300 ml with a Teflon liner of 140 ml and 233 ml, respectively.

Hydrothermal Synthesis Conditions *__200 ml__ Steel body with a Teflon liner of __140 ml__*				
Series Number	**Parameters**			
	T(ºC)	**[V^{5+}] (mol/l)**	**t (h)**	**f (%)**
1	161 | 185 | 199 | 212 | 226 | 238	0.0971	8	42
2	238	0.0486 | 0.0971 | 0.1460	8	30
3		0.0971	8 | 72 | 120	30
4			8	30 | 42
__200 ml__ and *__300 ml__ Steel body with a Teflon liner of __140 ml__ and __233 ml,__* respectively				
5	238	0.0971	8	30

2.3. Synthesis of VO_2(M)

Two different routes have been explored in order to synthesize VO_2(M) nanostructures. The first one consisted of a two-step hydrothermal synthesis from a VO_2(A) and VO_2(M) mixture, while the second one involved a transformation from VO_2(B) into VO_2(M) through a simple heating in a tube furnace.

2.3.1. Two-Step Hydrothermal Treatment

In a typical synthetic route for transforming VO_2(A) with a small portion of VO_2(M) into only VO_2(M), 0.4792 g of the VO_2(A) powder containing a small amount of VO_2(M) phase, and previously synthesized through hydrothermal treatment, was dispersed into 70 ml of deionized water with magnetic stirring at 1000 rpm, during 15 min. The mixed black solution was transferred into a 300 ml stainless steel

autoclave with a 233 ml Teflon liner. The autoclave was sealed and maintained at 238 ºC for 24h and then naturally cooled down to room temperature. The products were collected and washed several times by centrifugation and with deionized water and absolute ethanol at 2500 rpm for 30 min, in order to remove any possible residues. Finally, they were dried in an oven at 80 ºC for 15 min.

2.3.2. Conventional Heating Treatment/Calcination

In order to transform VO_2(B) into VO_2(M), about 0.4 g of VO_2(B) nanostructures, which were previously synthesized through hydrothermal treatment, were heated at 700 ºC for 2h in a tube furnace and cooled down to room temperature with 5 ºC/min heating/cooling rate. This calcination has been conducted under a high purity Ar (argon) atmosphere (99.999%) to prevent the oxidation of the sample.

2.4. Characterization Methods

2.4.1. XRD

Samples of VO_2 nanostructures obtained by hydrothermal synthesis were characterized by X-ray diffraction (PANalytical X'Pert) with Cu *Kα* radiation (*λ* = 1.540598 Å) at 40 kV and 30 mA, with the linear detector X'Celerator. The diffraction patterns were collected in Bragg-Brentano configuration in 2*θ* ranging from 10° to 60° with a 0.0167º step size and 140 s per step. The phase purity of the samples was checked by comparing the experimental XRD patterns to standards compiled by the Joint Committee on Powder Diffraction and Standards (JCPDS). The sample holder used to measure the powder was a glass coverslip, given origin to the slight curve between 15° and 25° (2*θ*) present in some diffractograms. This curve represents the amorphous signature of the glass.

2.4.2. HT-XRD

The above-mentioned XRD diffractometer was further used with a high temperature (HT-XRD) chamber under air flow in order to study the stability, oxidation resistance properties and phase transition of VO_2(B). The powder of VO_2(B) was placed on the strip of an Anton Paar high-temperature chamber and the HT-XRD patterns were acquired using 0.033 º and 149 s per step under the air between 25 ºC and 400ºC.

2.4.3. SEM-EDS

The scanning electron microscopy (SEM) was used to observe the morphology of the synthesized VO_2 nanostructures, using the field emission scanning electron microscope of high resolution (ZEISS Supra-55VP FEG SEM), equipped with a field emission gun (SEM-FEG) at an acceleration voltage of 1 kV. Images were analyzed with Image J (version 1.48v, http://imagej.nih.gov/ij/)) in order to achieve a statistical estimation of the dimensions (length/width and some thicknesses) of the VO_2 nanostructures obtained.

2.4.4. ATR-FTIR

ATR-FTIR (attenuated total reflection - Fourier transform infrared spectroscopy) has been used to characterize the nanostructures. The measurements were performed in a Perkin Elmer Spectrum 100 spectrophotometer with the ATR system to identify the chemical species formed. When measuring solids by ATR, it is essential to ensure good optical contact between the sample and the germanium crystal. Germanium has, by far, the highest refractive index of all the ATR materials available. This means that the effective depth of penetration is approximately 1 µm. For most samples, this will result in a weak spectrum. However, this is an advantage when analyzing highly absorbing materials.

To get the infrared spectrum of a sample it is necessary to collect spectra of the sample and a "reference" (or "background"), which makes it possible to eliminate the environment influence, since the sample transmission spectrum is divided by the reference transmission spectrum. Each spectrum was obtained in the wavenumber range 4000-400 cm^{-1} by averaging 400 scans at a 4 cm^{-1} resolution in order to obtain a suitable S/N ratio.

Spectra were acquired on samples of VO_2(B), VO_2(A) and a mixture of VO_2(A) and VO_2(B). The results were compared with the data published in the literature.

2.4.5. Raman Spectroscopy

Raman shift provides information about vibrational, rotational and other electric level transitions in molecules. Certain vibrations that are allowed in Raman are forbidden in IR, whereas other vibrations may be observed by both techniques, but with significantly different intensities. Thus, these techniques can be used in a complementary way. To enable the identification of the synthesized phase or the investigation of the modifications in the crystal structure induced by intense light beams, Raman spectra of VO_2(B) and VO_2(A) were conducted on Renishaw in Via Raman RGH22 microscope coupled to a Leica DMLM microscope. An argon-ion laser beam with a nominal power of 0.5 mW was focused by a x100 lens. During the measurements, it was also used a power of 10% of the nominal power (0.05 mW). The full spectrum was obtained in 60 s. The heating of the VO_2(A) sample by laser beam was carried out with a power of 5 mW (10x the nominal power), during 6 s.

2.4.6. TG-DTA or TG-DSC

Transitions phase temperature was measured by a complete modular thermal analysis platform (LABSYS EVO TG/DTA/DSC - differential thermal analysis and differential scanning calorimetry) under inert/reducing (argon) or oxidizing (air) atmosphere using a heating/cooling rate of 5 ºC/min between room temperature and 700 ºC. The furnace temperature is regulated by means of an S-type thermocouple (Pt / Pt Rh 10%) located in the furnace.

3. Results and Discussion

3.1. Influence of the Hydrothermal Synthesis Parameters

Along this dissertation/section, the effects of four hydrothermal parameters (the synthesis temperature, the V^{5+} concentration in solution, the synthesis time and the filling percentage) were investigated, more precisely through the 200 ml Teflon-lined autoclave. The following results, and respective analysis, describe the role of each parameter on the formation of VO_2 nanostructures.

3.1.1. Synthesis Temperature

The study of synthesis temperature influence, Series 1 (**Table 2.2.2**), was performed by varying the synthesis temperature from 161 ºC to 238 ºC and by keeping constant the process time at 8h for a filling percentage of autoclave 42%. **Figure 3.1 and 3.2** show how the structure and morphology of VO_2 are influenced by these parameters.

Figure 3.1 shows the diffraction patterns of the as-obtained samples as the temperature ranges from 161 ºC to 238 ºC and the JCPDS of VO_2(B), VO_2(A) and $V_3O_7H_2O$ for comparison purposes.

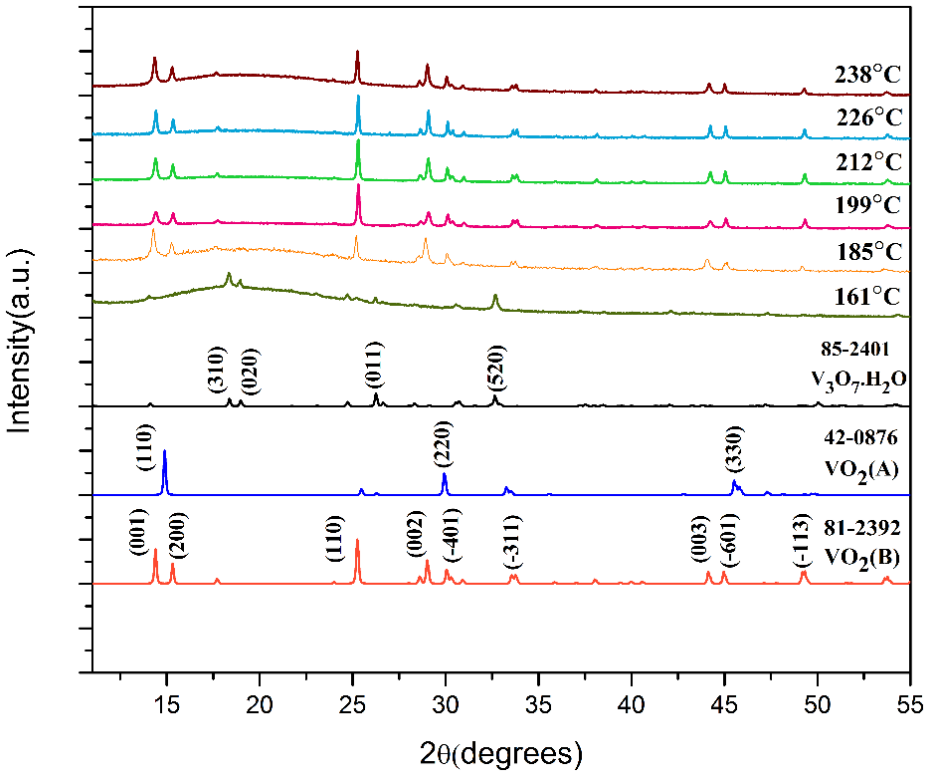

Figure 3.1. XRD patterns for the samples synthesized at different temperatures with process duration of 8h being the autoclave filled at 42% (Series 1).

Diffraction patterns represented in **Figure 3.1** show that all the samples obtained are well crystallized. As for the system temperature at 161 ºC, no other peaks could be indexed, except for those belonging to $V_3O_7.H_2O$ (JCPDS#85-2401).

With the temperature increasing from 161 ºC to 238 ºC, peaks of $V_3O_7.H_2O$ disappear, while the peaks belonging to monoclinic VO_2(B) (JCPDS#81-2392), with lattice parameters of *a* = 12.09 Å, *b* = 3.70 Å, and *c* = 6.43 Å, appear, with the main direction of growth (110), since the relative intensity of (110) peak is stronger than those of the JCPDS pattern.

Pure VO_2(B) was obtained when the hydrothermal treatment temperature was higher than 185 ºC, while lower temperature was beneficial for the formation of $V_3O_7.H_2O$ phase. This result is consistent with literature, since Shidong Ji et al. [14] and Huang et al. [43] have shown that VO_2(B) phase is often obtained at the temperature of 180 ºC. Shidong Ji et al. further state that VO_2(B) is always firstly formed and, with the extension of hydrothermal treatment time, other polymorphs, derivative forms of VO_2(B), appear. Moreover, Shidong Ji et al. [14] describe system pressure as a very important factor, since it presents a great influence on the formation of the final VO_2 polymorphs. Galy [44] reports that VO_2(A) strongly depends on the pressure during synthesis. No peaks belonging to VO_2(A) could be found in these XRD patterns. Regarding the results and the authors' conclusions, probably 8h of synthesis is not enough time to reach the necessary pressure to form VO_2(A), even with a higher temperature.

The morphology and size of the resulting VO_2 products are shown in **Figure 3.2.** Firstly, it was interesting to note that the appearance of VO_2(B) compounds and $V_3O_7.H_2O$ were obviously different. For example, VO_2(B) powder was black with nice dispersity, while $V_3O_7.H_2O$ powder was green and the density paper-like could be formed preferably after centrifuge and drying.

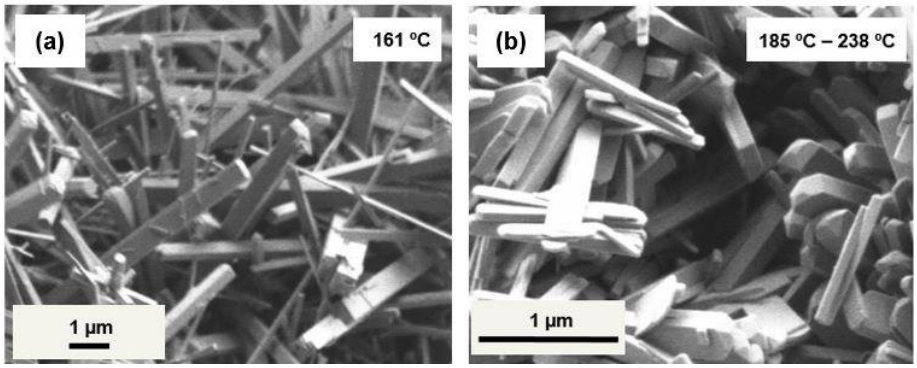

Figure 3.2. Series 1 samples' SEM images.
Samples formed at varying temperatures for holding 8h with a filling percentage of 42%: (a) 161°C; (b) temperatures from 185°C to 238°C.

SEM images show a difference in the morphology of the sample obtained at 161 ºC and the ones obtained in the range from 185 ºC to 238 ºC. VO_2(B) has a homogenous phase (**Figure 3.2 - b**) with particles uniformly sized, forming nanostructures that resemble a belt, with 0.861 - 1.154 µm in length and about 0.140 - 0.226 µm in width. This morphology was kept unchanged for the different synthesis temperatures in the range from 185 ºC to 238 ºC, as well as the size, that did not change significantly. The belt-like particles of VO_2(B) are consistent with the literature reports [11], [45]. The relatively high length-width ratio (4.81) of the obtained VO_2(B) belt-like nanostructures indicate a growing kinetics of the VO_2(B) phase, since they are all different in those three dimensions.

The morphology of the $V_3O_7.H_2O$ phase formed at 161 °C is very different from VO_2(B), which appeared as the belt-like particles with a rectangular section (**Figure 3.2 - a**), approaching to nanorods with higher poli-dispersion of dimensions.

Combining XRD and SEM results, and according to Xu H.F. et al. [11] analysis, during synthesis vanadium pentoxide was firstly dissolved and hydrated, which formed diverse species, such as VO_2^+, ultimately reduced by $H_2C_2O_4$. These species were further reduced and formed VO_2 as the system temperature increased. Thus, when the reaction temperature is lower than 180 ºC, those species are not sufficiently reduced to form VO_2(B), giving rise to $V_3O_7.H_2O$. Considering the similar shapes and sizes between the samples synthesized at the temperature range from 185 ºC to 238 ºC, synthesis temperature has a limited effect over the morphology of the obtained VO_2(B) nanostructures in these experiments.

3.1.2. V^{5+} Concentration in Solution

To study the influence of V^{5+} concentration in solution the varied parameters are those indicated in **Table 2.2.2**, Series 2 samples. The temperature was kept at 238ºC for 8h and the autoclave was filled at 30%. The crystal structure and morphology of the as-obtained samples are shown in **Figures 3.3 and 3.4**, respectively.

Figure 3.3 shows the XRD patterns for samples obtained with three different V^{5+} concentrations, and it also includes the JCPDS patterns of VO_2(A), VO_2(B) and $V_3O_7H_2O$ for comparison.

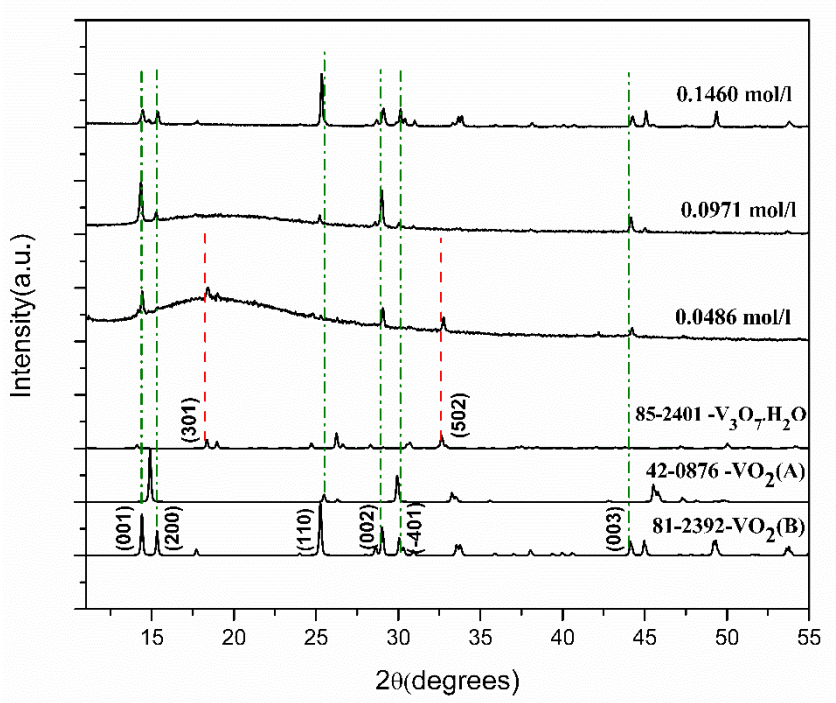

Figure 3.3. XRD patterns for samples synthesized according to different V^{5+} concentrations (Series 2).

As shown in **Figure 3.3.**, for the lowest concentration of V^{5+} used, 0.0486 mol/l, the diffraction pattern exhibits a mixture of peaks of $V_3O_7.H_2O$ (JCPDS#85-2401) and VO_2(B) (JCPDS#81-2392). Pure VO_2(B) was obtained when the concentration was higher than 0.0971 mol/l but, when the concentration rises to the highest value used, 0.1460 mol/l, the (110) diffraction peak's intensity increased, and (001) peak's intensity decreased, approaching to the typical powder diffraction pattern of VO_2(B).

High pure VO_2 compounds can be reached with a careful control of V_2O_5 to oxalic acid molar ratio. Even with the increase of the concentration in solution, molar ratio was kept at 1:3.

Results about the effects of the V^{5+} concentration in solution on the formation of VO_2(B) phase were not found in the literature. Preliminary experiments have revealed that solutions prepared with a molar ratio ($V_2O_5/H_2C_2O_4$) 1:1 and 1:2 exhibited orange and green colors, respectively, meaning that vanadium in the solution was not completely reduced. Interestingly, the solution prepared with a V^{5+} concentration of 0.0486 mol/l, even with a molar ratio 1:3, also exhibited a green color, which may explain the presence of $V_3O_7.H_2O$ and VO_2(B) mixtures in XRD patterns. On the other hand, higher concentration solutions exhibited a dark blue color, indicating the reduction of vanadium in solution and forming VO_2(B) phase after hydrothermal treatment.

VO_2(A) phase can be obtained by using the same V^{5+} concentration in solution, but after a longer time or under a higher pressure in the hydrothermal treatment.

The morphology of synthesized powders of Series 2 samples shown in **Figure 3.4** reveal that the microstructure is remarkably influenced by the V^{5+} concentration.

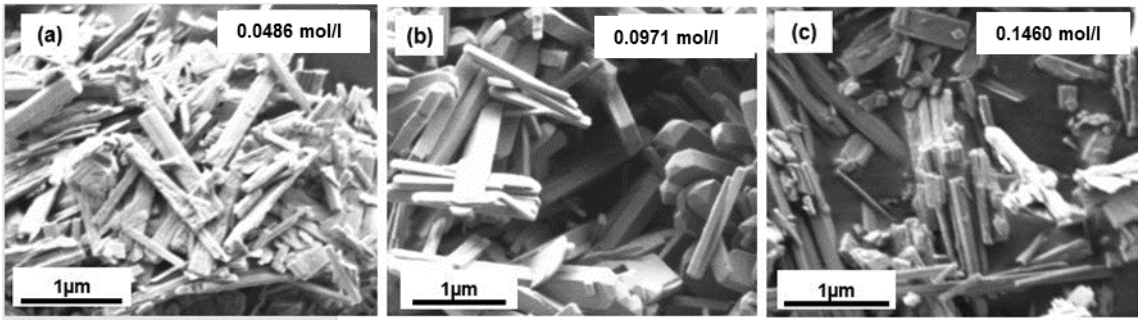

Figure 3.4. Series 2 samples' SEM images.
Samples formed according to different V^{5+} concentrations in solution for holding 8h with a filling percentage of 30%: (a) 0.0486 mol/l; (b) 0.0971 mol/l; (c) 0.1460 mol/l.

By combining the XRD results and the **Figure 3.4 – b,** we can conclude that VO_2(B) is formed when the concentration is about 0.0971 mol/l, appearing as belt-like powders, 1.107 µm in length and about 0.192 µm in width. **Figure 3.4 - a** shows a mixture between the belt-like morphology from VO_2(B) and the belt-like particles with a rectangle section from $V_3O_7.H_2O$. **Figure 3.4 – c**, which corresponds to the highest concentration, exhibits an aggregation of nanostructures. According to the XRD patterns, this concentration also promotes the growth of VO_2(B), despite the fact that the morphology, and comparatively to the concentration of 0.0971 mol/l, shows an agglomeration of belt-like nanoparticles and an uneven and irregular surface. It is possible to interpret this as resulting from different levels of supersaturation. At a higher concentration, there might be more chances to form additional seeds on the surface of the preformed crystal, which leads to the formation of multiple armed VO_2(B) microcrystals. In contrast, a lower concentration of vanadium would favor the formation of fewer seeds, thus making the crystals grow longer and with a smooth surface. When the V^{5+} concentration in the solution is too high, hydrothermal reaction parameters, such as time and temperature, could probably have not effectively dissolved the metastable VO_2(B) phase.

3.1.3. Synthesis Time

To understand the mechanisms of the transformation occurred from VO_2(B) into VO_2(A), experiments (Series 3- **Table 2.2.2**) were carried out at 238 ºC for different holding periods during the hydrothermal treatment and under the filling percentage of 30%.

Figure 3.5 shows the XRD patterns for samples synthesized during different periods of time, being also indicated the JCPDS ones for VO_2(A) and VO_2(B).

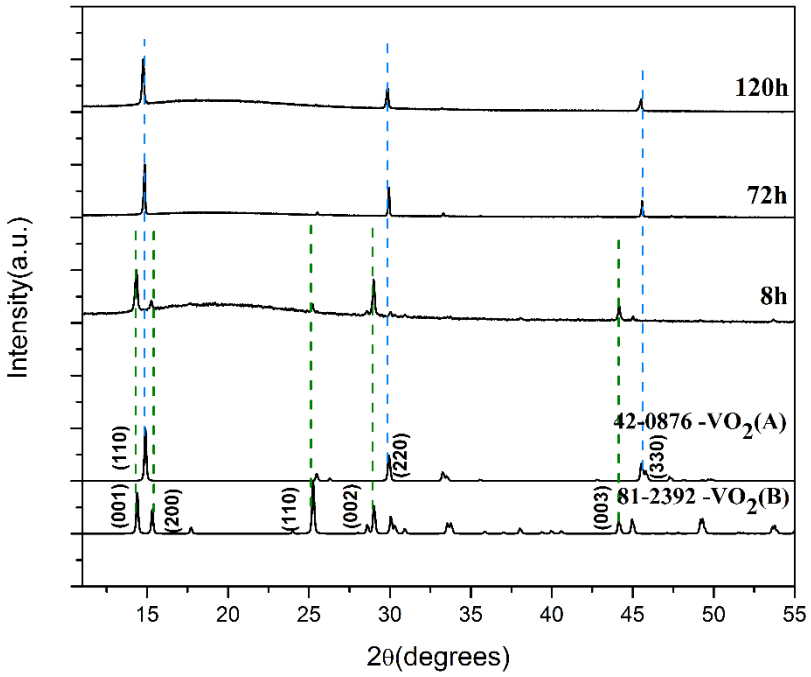

Figure 3.5. XRD patterns for samples synthesized at 238°C for different holding periods (Series 3).

XRD patterns of **Figure 3.5** clearly show that the 8h synthesis leads to samples with a similar structure to VO_2(B) (JCPDS#81-2392). However, it also shows that other polymorphs, derivative from VO_2(B), and with the extension of hydrothermal process duration, lead to a VO_2(A) phase (JCPDS#42-0876) with lattice parameters of $a = b = 8.45$ Å, and $c = 7.68$ Å.

Thus, if the reaction takes longer, at least 72h, and according to the study performed, VO_2(B) phase is transformed into VO_2(A). After 120h of treatment, no other phases besides VO_2(A) were found. Meanwhile, the diffraction intensity of VO_2(A) phase, holding for 120h, gradually decreased in contrast to VO_2(A) holding for 72h, which could indicate the further growth of a new VO_2 phase or it could be just due to a lack of powder during the measurement.

From the thermodynamics' point of view, metastable VO_2(B) will transfer to VO_2(A) with the extension of the holding time at certain temperatures or by simply increasing the temperature. Since the system used to perform the hydrothermal treatment presents a maximum working temperature of 250 ºC, it was only possible to study the effect of holding time at the highest allowed temperature. The formation of VO_2(A) should be initiated with the assembling of VO_2(B) belt-like nanoparticles and followed by a crystal structure adjustment. The formation of new phases of VO_2, such as VO_2(M) and VO_2(R), was reported by Shidong Ji et al. [3], [22], [39]. The authors reported VO_2(B) as an intermediate phase for the

formation of further phases, such as VO_2(M) and VO_2(R). These phases are very dependent on the temperature, since they are formed at temperatures greater than 260 ºC.

Shidong Ji et al. also reported the role of the pH on the formation of the new phases, concluding that, when the initial pH of the solution decreased, VO_2(R) phase was obtained in a shorter period of time. Since the influence of this parameter was not studied during the development of this work, the combination between time and temperature carried out by Series 3 was certainly not sufficient to generate the transformation from VO_2(A) to VO_2(M) or VO_2(R).

SEM images (**Figure 3.6**) are used to compare both VO_2(B) and VO_2(A) phases' morphology.

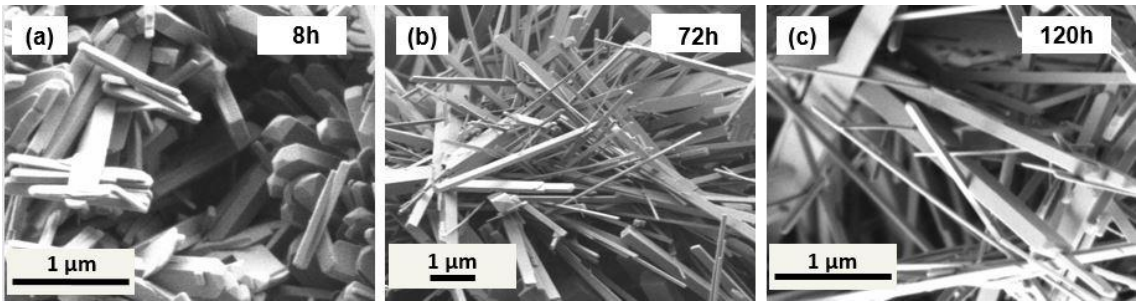

Figure 3.6. Series 3 samples' SEM images.
Samples synthesized at 238°C with the filling percentage of 30% for different holding times: (a) 8h; (b) 72h; (c) 120h.

Figure 3.6 - **a** shows the metastable VO_2(B) with the typical belt-like morphology, which is the usual morphology of VO_2(B) according to what has been reported by other researchers (**Appendix 1**). On the other hand**, Figures 3.6 – b and - c** show that VO_2(A) appeared as a mixture of nanorods and nanowires containing a rectangular section. In spite of the hybrid morphology, the rod-like morphology of VO_2(A) is compatible with the ones reported in literature [11]. These results show that VO_2(A) exhibits poly-dispersion of section dimensions and lengths, as the widths vary from 0.086 µm and 0.192 µm. This suggested that the morphology of the previously obtained VO_2(B) nanostructures was partly preserved during the ongoing reaction process. The length of the as-obtained particles, with values around 4.274 µm, did not change significantly for samples synthetized between 72h and 120h. SEM images in **Figure 3.6** also show that metastable VO_2(B) and VO_2(A) phases were preferentially grown along some particular crystal directions. Time has an important role on the VO_2's nanostructures phase transformation during hydrothermal treatment. However, results have shown that no other phases than VO_2(A) could be yielded, even by extending the reaction time from 8h to 120h days in a relatively low temperature environment.

3.1.4. Filling Percentage

As the hydrothermal process depends on the pressure inside the chamber, the filling percentage also influences the products formed, more precisely due to a relationship between filling percentage and auto-generated pressure. In fact, the results reported in literature [44], [46] show that this parameter has a great influence on the final VO_2 polymorphs. In order to evaluate the influence of the pressure, Series 4, described in **Table 2.2.2,** were prepared at 238 ºC for 8h, where two filling percentages were compared.

The XRD patterns of samples prepared with filling percentages of 30% and 42%, as well as the JCPDS patterns of VO_2(A) and VO_2(B), are shown in **Figure 3.7.**

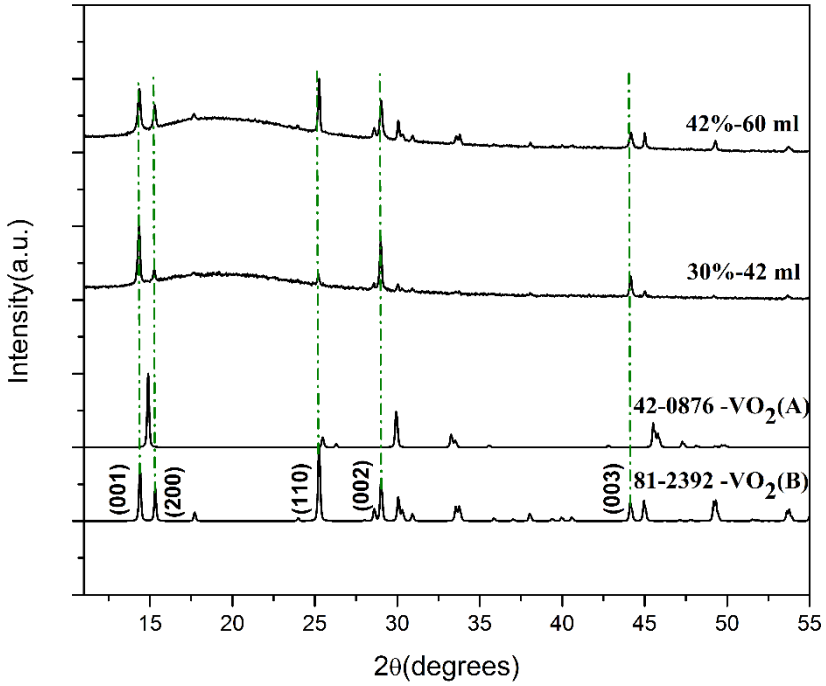

Figure 3.7. XRD patterns for samples prepared with different filling percentages (Series 4).

Figure 3.7 shows that there is no other phase than VO_2(B) (JCPDS#81-2392), even when the filling percentage increased from 30% to 42%. However, some differences in the peaks can be seen: the intensity in direction (001) and (002) decreases, while the intensity in direction (110) and (200) is enhanced when the pressure increases. In fact, with higher pressure, the XRD pattern of the VO_2 products is closer to the VO_2(B) phase. Regarding the present results, some conclusions can be taken: the increase of pressure was not enough to promote the conversion of VO_2(B) into other polymorph, even if we consider the highest temperature used. This assumption can be supported through the fact that, when the filling percentage increased from 30% to 42%, the pressure inside the autoclave raised from 17 bar to 20 bar. This means that the gain was insufficient to promote the phase transformation, despite the fact that it has promoted the achievement of a pure VO_2(B) phase. Following the basic reaction inside the autoclave, some authors [14] revealed that VO_2(B) transforms into VO_2(A) and that this last transforms into other polymorphs under high pressures, which is promoted by a filling percentage of at least 60% combined with a temperature higher than 270 ºC during at least 24h. Then, it was also made an attempt to study this effect by using a higher volume autoclave: 300 ml instead 200 ml.

The morphology of the samples obtained with different filling percentages can be observed in the SEM images in **Figure 3.8**.

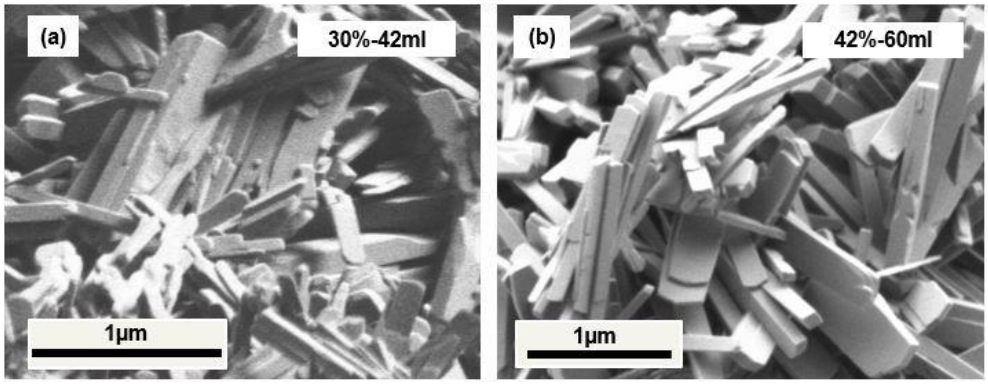

Figure 3.8. Series 4 samples' SEM images.
Samples synthesized at 238°C for holding 8h with different filling percentages: (a) *f* (%) = 30%; (b) *f* (%) = 42%.

As seen in **Figure 3.8 - a**, the sample synthesized with the filling percentage of 30% exhibited similar one-dimensional belt-like morphology, with an average 0.833 µm in length and 0.175 µm in width. However, it is possible to observe an aggregation of belts and a surface with some seeds. Due to the original small sizes and high surface energy, the spontaneous stacking of these small VO_2(B) nanostructures could occur. Similar anomalously assembled structures were also observed in the SEM images of Series 2, as shown in **Figure 3.4 – c**. On the other hand, when the filling percentage increases to 42%, seeds disappear and the morphology shows uniform belt-like nanostructures, the typical VO_2(B) morphology with an average of 1.107 µm in length and 0.192 µm in width. This could mean that the anomalous assembly of thin VO_2(B) nanostructures could be an intermediate to achieve intimate interfacial stacking and later develop into longer belt-like micro and nanostructures. Since there is a slight difference between the pressures inside the autoclave, a lower pressure could generate a high surface energy on the VO_2(B) nanostructures and, consequently, promote its aggregation until the rise of the anomalous nanostructures.

In order to study the influence of the hydrothermal synthesis conditions, on the final VO_2 nanostructures, when taken to the extreme regarding two different filling percentages (30% and 60%), Series 6 was carried out (**Appendix 4** – **Table A4.1**). The results and the respective analysis of these tests can be found next.

Series 6 was carried out at extreme conditions in order not just to study the influence of the hydrothermal synthesis conditions when these are taken to the extreme but also to analyze the effect of the filling percentage when it varies from 30% to 60%. These additional experiments were performed through the 300 ml autoclave.
In this experiment, the system pressure was controlled by varying the filling percentage, while the remaining parameters that were taken to the extreme were kept constant. The corresponding XRD patterns are shown in **Figure 3.9.**

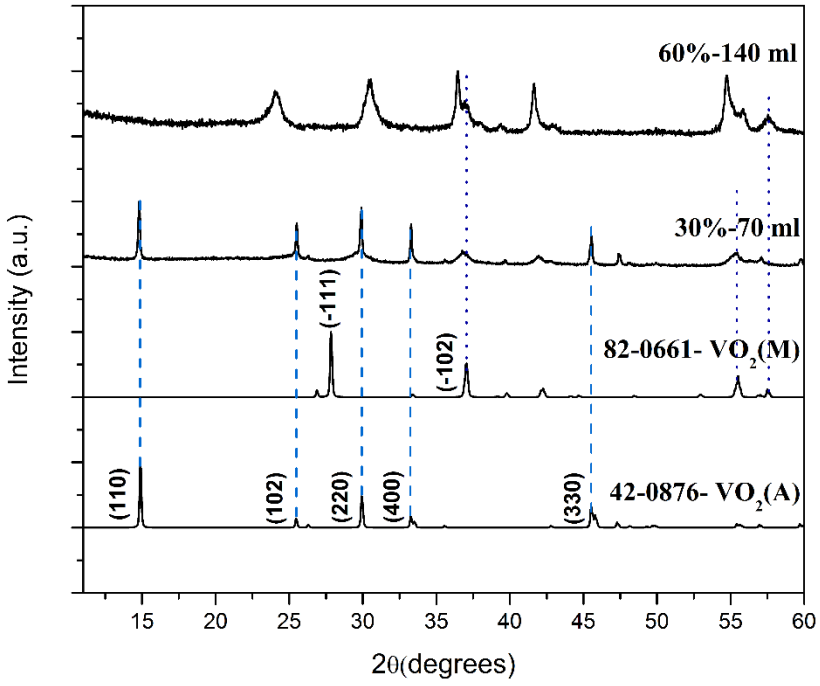

Figure 3.9. XRD patterns for samples prepared through the 300 ml Teflon-lined autoclave, at 238 ºC for 120h with filling percentages varied from 30% to 60% (Series 6).

As previously described, auto-generated pressure became high with the increase of the filling percentage or the increase of the temperature. When the filling percentage was 30%, at this conditions, diffractograms in **Figure 3.9** show a VO_2(A) phase with some crystallinity problems, since some peaks are large, and some unidentified phases are noticed, which can be derived from intermediate VO phases formed during the treatment. When the filling percentage increased from 30% to 60%, the pressure inside the autoclave also increased from 35 bar to 55 bar. This is a significant difference, which promotes the growth of non-crystalline VO_2 derivatives. Although, the peaks represented in **Figure 3.9** also show that a very limited amount of VO_2(M) appeared. Authors that studied this behavior [14], [46] show that, when the pressure inside the autoclave increased, for example from 40% to 60% or from 60 ml to 80 ml, VO_2(B) will transform into VO_2(A), which consequently transforms into VO_2(R/M). Under the inducement of high pressure, the formation of interfacial covalent bonds assists the synergistic recrystallization to transform VO_2(B) into VO_2(A). In this regard, the formation of these nanostructures was based on an oriented attachment recrystallization mechanism.

Shidong Ji et al. [14] present many explanations about the reactions that happen inside the autoclave under high pressure. Authors explain that, for water, there is a critical filling percentage, which depends on temperature in hydrothermal treatment. Extreme high pressure would be caused by the expansion of liquid water, more precisely when the filling percentage is higher than the critical one, and in the absence of vapor phase. On the other hand, when the filling percentage is lower than the critical one, the liquid water phase and vapor water phase should coexist in the autoclave. In this case, the saturated pressure in the autoclave depends only on the temperature.

It is possible to calculate these data from some database, such as ‘‘International Saturated Steam”. As the authors have done, the equilibrium pressure when the temperature of reaction is 238 ºC can be taken from that database. In this case, the equilibrium pressure for that temperature is 31.29 bar.

Table 3.1 shows the practical pressure that was measured by heating the 300 ml Teflon-lined autoclave at 238 ºC using deionized water and real solution separately with different filling percentages (30% and 60%).

Table 3.1. Pressure in autoclave after heating water and real solution at 238 ºC for 120h.

Autoclave	**Item**	***f (%)* = 30%**	***f (%)* = 60%**
300ml	Pressure for water (bar)	*25.*	*26*
	Pressure for real solution (bar)	*35*	*55*

According to the data presented in **Table 3.1**, for water, and in this work, the measured values are also close to the reference value. The difference between these values for 30% and 60% filling percentage is not significant. When the filling percentage is 60%, the pressure did not surpass the reference pressure for water, which means that 60% of filling did not exceed the critical filling percentage for water at 238 ºC. On the other hand, for real solution it is possible to observe that, when the synthesis is carried out at these extreme conditions, both of the filing percentages (30% and 60%) exceed the critical one. As the authors have explained, the real reaction system in these experiments is divergent from pure water. **Equation 2** shows the main reaction in the experiments of the present work, more properly, during hydrothermal treatment for the formation of VO_2:

Equation 2

$$V_2O_5 + H_2C_2O_4 = 2VO_2 + H_2O + {}_2CO_2 \uparrow$$

The chemical reagents and their reaction made this complex system and the auto-generated pressure during hydrothermal treatment seemed unsolvable through calculation. The elevation of pressure for real system would be considered as the contribution of the CO_2 produced following the previous reaction. The solubility of CO_2 mainly depends on temperature and pressure. With the increase in filling ratio, and subsequently increase in pressure, the generated amount of CO_2 increases and the volume accommodating the vapor phase decreases. So, the elevation of pressure could be observed when the filling ratio increases.

Since the pressure in these experiments was too high, the peaks in **Figure 3.9,** that at the beginning could be attributed to intermediate VO_2 phases, may now be attributed to the CO_2 absorbed on the surfaces of the nanostructures. Another explanation can be related to the formation of oxide-hydroxide of vanadium during the synthesis process. XPS, FTIR or Raman characterization of this sample could give a confirmation about these suppositions.

In summary, when the hydrothermal synthesis conditions are taken to the “limit” through a 300 ml Teflon-lined autoclave, contributing to a super-high pressure inside the cup, they give rise to non-crystalline and anomalous VO_2 nanostructures.

SEM images can be consulted in **Figure 3.10**, where it is possible to observe nanowires when the filling percentage was 30% (**Figure 3.10 - a**), which corresponds to VO_2(A) traditional morphology. On the other hand, **Figure 3.10 - b** shows an anomalous morphology with very-agglomerated micro-spheres and some structures that reassembles snowflakes.

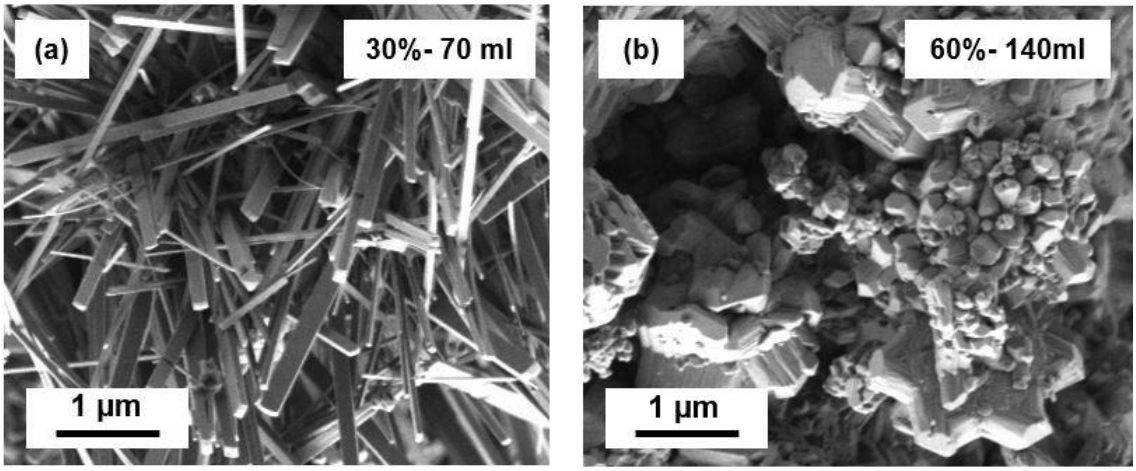

Figure 3.10. Series 6 samples' SEM images.
Samples synthesized at 238 ºC for holding 120h with different filling percentages: (a) *f (%)* = 30%; (b) *f (%)* = 60%.

Both of these types of morphologies (snow flake aggregation and quasi-spherical nanostructures) are coherent with VO_2(M) morphology (**Appendix 1-Figure A1.2 - c**). However, and in spite of this coherency, it may also have been obtained an intermediary phase between VO_2(A) and VO_2(M). The morphology of the 60% filling percentage sample can be explained by the analysis developed above. Combining SEM and XRD results, the emergence of few VO_2(M) microstructures on the samples synthesized with a filling percentage of 60% is understandable. To have access to more information about the effect of high pressure parameter in hydrothermal technique, consult the literature [14], Chapter 3.3: *Thermodynamic analysis for the pressure related phase transformation.*

All the results obtained so far are very dependent on the system used to carry the synthesis, namely on volume of the autoclave used. To demonstrate this theory, some additional essays have been made in order to prove that, when hydrothermal synthesis are performed in the same conditions, the results can be very dissimilar, more precisely when a different system is applied.

3.2. Modifications on the Hydrothermal Synthesis Process

According to the existing literature, several experiments have been developed in order to study the influence of some conditions on the formation of VO_2 nanostructures, namely the absence of Teflon liner, autoclave's volume, effect of non-stirring, and the presence of a Si substrate during the synthesis.

3.2.1. Influence of Teflon-lined Autoclave System

3.2.1.1. Influence of Teflon-liner Absence

This study was carried out through the 200 ml Teflon-lined autoclave in order to evaluate the role of the Teflon vessel presence during the hydrothermal synthesis (Series 7, **Appendix 4 – Table A4.2**). Samples were synthesized at 238 ºC for 72h with a filling percentage of 30%, with and without Teflon vessel. The obtained XRD results are shown in (**Figure 3.11)**. Indeed, it is quite notable that there is a difference between samples synthetized with and without Teflon vessel.

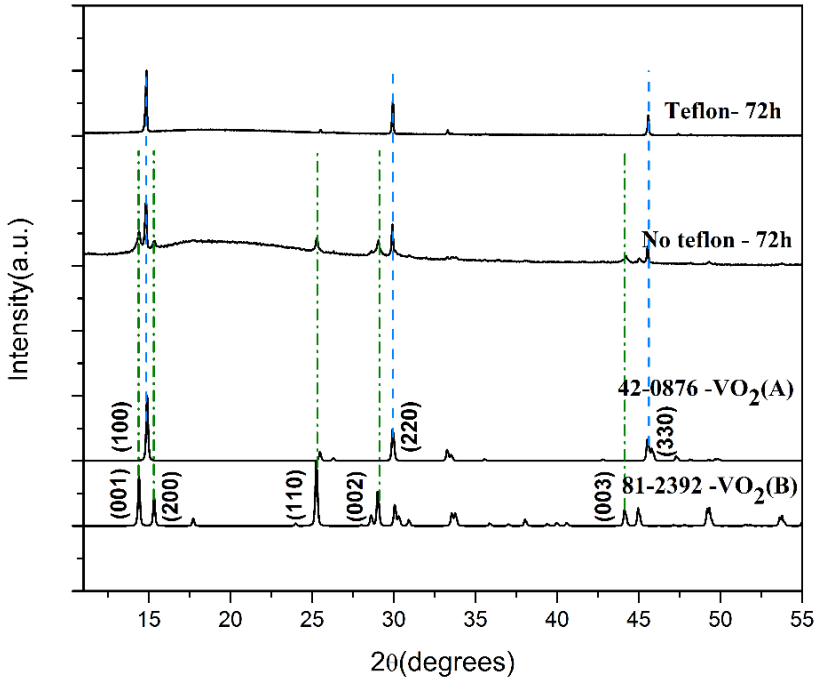

Figure 3.11. XRD patterns for samples synthesized through 200 ml steel body autoclave at 238ºC for holding 72h with a filling percentage of 30% with and without Teflon vessel (Series 7).

When the Teflon vessel is not present during the hydrothermal synthesis, only a mixture of VO_2(B) and VO_2(A) is resulting, while when the Teflon is present, same hydrothermal synthesis conditions lead to the formation of single VO_2(A) phase. It is noticed that the morphology of the sample when the Teflon vessel was not used (**Figure 3.12 - a**), is an agglomerated mixture of belt-like nanostructures and nanowires (VO_2(B) and VO_2(A) phases). On the other hand, the morphology of the samples synthesized with Teflon vessel (**Figure 3.12 - b**) represents VO_2(A) nanowires with well-defined sizes (4.274 µm in length and 0.195 µm in width). SEM results (**Figure 3.12**) are coherent with the observations and analysis of the respective XRD patterns.

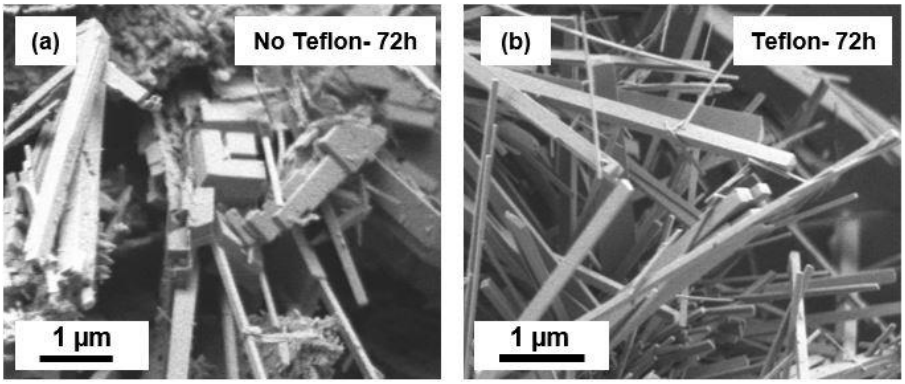

Figure 3.12. Series 7 samples' SEM images.
Samples synthesized through 200 ml steel body, in order to study the influence of the Teflon vessel absence, at 238 ºC for holding 72h with a filling percentage of 30%: (a) synthesis performed without Teflon vessel; (b) synthesis performed with Teflon vessel.

Teflon vessel has played a great role during the hydrothermal synthesis when carried out through a steel body autoclave system. It was interesting to notice that when the Teflon vessel was not present, at the end of the hydrothermal synthesis, some part of the compound was stuck on the autoclave steel walls, which means that nucleation points were created, promoting the growth of non-homogenous VO_2 phases during the treatment processes. In this way, Teflon vessel purpose is not just to protect the steel walls from acid solutions but also to avoid nucleation points on steel.

3.2.1.2. Influence of Autoclave Type (200 ml and 300 ml)

Synthesis time, temperature and filling percentage have a great influence on the formation of VO_2 nanostructures. However, these parameters may depend on the system used to perform the syntheses. The aim of this section is to compare the influence of different Teflon-lined autoclaves volumes: 200 ml and 300 ml in capacity (Series 5- **Table 2.2.2**).
XRD patterns (**Figure 3.13**) show the effects of the autoclave's volume on the formation of VO_2 nanostructures.

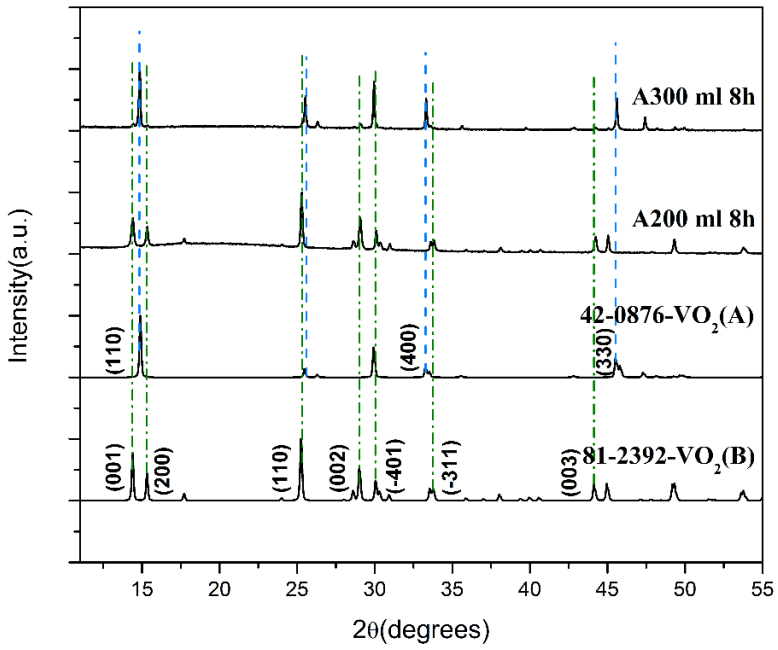

Figure 3.13. XRD patterns for the samples synthesized through two different autoclaves (200 ml and 300 ml) at 238°C for 8h with a filling percentage of 30% (Series 5).

As shown by the XRD patterns (**Figure 3.13**) a pure VO_2(B) (JCPDS#81-2392) phase is obtained when the reaction is performed in a 200 ml autoclave (similar to the results of **Figure 3.1**). A higher volume autoclave is used to carry the same synthesis, keeping the same conditions, and a mixture between VO_2(B) and VO_2(A) emerges. The influence on the samples' morphology is shown in the SEM images of **Figure 3.14.** VO_2(B)'s structure formed by such belt-like nanostructures (**Figure 3.14- a**) is the main characteristics of the synthesis products in the 200 ml autoclave. On the other hand, an agglomerate mixture of VO_2(B) nanostructures, similar to belts, and VO_2(A) nanowires (**Figure 3.14 - b)** are the products resulting from synthesis in 300 ml autoclave.

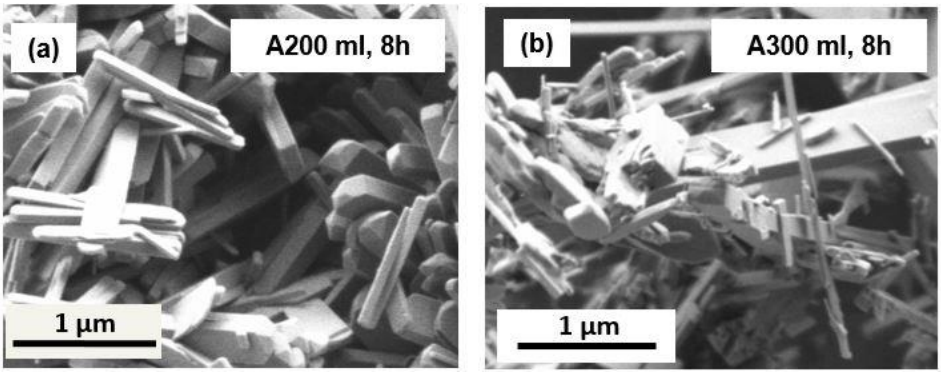

Figure 3.14. Series 5 samples' SEM images.
Samples synthesized in 200 ml and 300 ml steel body at 238°C for holding 8h with a filling percentage of 30%: (a) synthesis performed in the 200 ml autoclave; (b) synthesis performed in the 300 ml autoclave.

It is important to say that both of the steel bodies not only differ in volume but also in the thickness of their steel walls. Since the 300 ml steel body walls are thinner, the heating rate inside the cup is higher than the one felt inside the 200 ml autoclave. This could explain the obtained results, mainly the

formation of VO_2(A) with only 8h treatment. These results seem to be inconsistent with the ones obtained in the above section, when the presence of the Teflon liner in the 200 ml autoclave was tested, but in reality they are not: when the Teflon liner was not present, the heating rate inside the cup was higher than when the Teflon liner was present. This fact seems to show that a low heating rate inside the cup promotes the growth of VO_2(A), which is exactly the opposite of what is happening in the present section. Although the heating rate was lower with the presence of Teflon liner, it is not possible to compare two different heating rates when the conditions inside the cup were not kept the same. This means that the two different results obtained are due to the creation of nucleation points and when the Teflon liner is not present and not due to the heating rate. On the other hand, in the present section it is possible to compare and to affirm that, perhaps, the formation of VO_2(A) was due to the heating rate, since both of the autoclave were protected with the Teflon liner. Other possible explanation is the fact that, for the same filling percentage, the bigger autoclave corresponds to a higher absolute volume without solution. As such, the molecules within the solution could have a higher mean free path, which could create stronger collisions, changing, therefore, the monoclinic to tetragonal.

3.2.2. Effect on VO_2 Nanostructures' Morphology

In order to study the possibility to tune the morphology of the VO_2 nanostructures, two different approaches related with processing details were accomplished through the 300 ml Teflon-lined autoclave: the first one is related to the effect that non-stirring causes on the VO_2 nanostructures morphology, while the second one is associated to the use of a Si substrate as a structure directing template. Results of these experiments can be consulted throughout this section.

3.2.2.1. Influence of Non-Stirring

During all the hydrothermal synthesis developed in this work, the solution inside the cup has always been stirred at 1400 rpm. Previous results show that, when preferential conditions were carried, even with stirring, it was possible to obtain VO_2(B) phase with belt-structures. Therefore, it was decided to test the effect of this factor, using a 300 ml Teflon-lined autoclave at 238 ºC for 8h with a filling percentage of 30% (Series 8- **Appendix 4 – Table A4.3**).

XRD results (**Figure 3.15 - a**) show a mixture of phases: VO_2(B) (JCPDS#81-2392) and VO_2(A) (JCPDS#42-0876) with and without stirring. These results indicate that stirring has no influence on the final VO_2 structure, since the XRD patterns obtained with and without stirring are very similar.

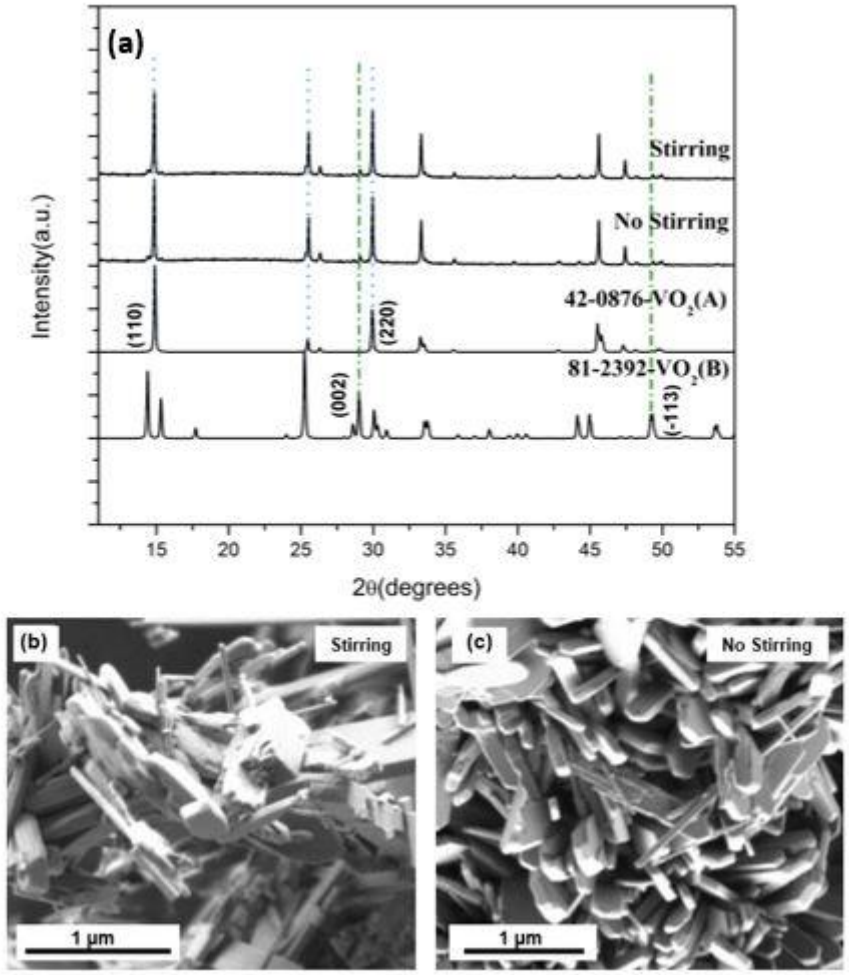

Figure 3.15. (a) XRD patterns for samples synthesized through 300 ml steel body autoclave at 238°C for holding 8h with a filling percentage of 30% with and without stirring (Series 8); (b-c) the corresponding Series 8 samples' SEM images, in order to study the influence of non-stirring on the morphology: (b) synthesis performed with stirring; (c) synthesis performed without stirring.

By observing the morphologies represented in SEM images (**Figure 3.15 b and c),** and at the first sight, it seems that non-stirring promotes a better belt-like nanoparticles and nanowires morphology, despite the fact that the previous results reported showed that even with stirring it is possible to obtain a suitable morphology. Perhaps, the system used to perform the synthesis allowed a higher temperature inside the cup when the external temperature felt during the experiment was higher (**Figure 3.15 - b**), promoting higher pressure inside and, consequently, an aggregation of the particles. The same conditions without stirring were accomplished when the external temperature was lower. Thus, the anomalous morphology obtained with stirring could be due to the used system and to the high temperature felt on the day that the experiment was performed. These observations show that the effect of stirring during the hydrothermal synthesis on the formation of VO_2 nanostructures is not relevant.

3.2.2.2. Effect of a Si Substrate on the Final Nanostructures' Morphology – An Innovative Experience

The use of a Si substrate during the hydrothermal treatment of VO_2 nanostructures was hardly ever reported in the literature, being this chapter considered as a brand new study. With the aim to tune VO_2 nanostructures morphology a Si substrate orientated <100> (10 x 10 mm^2) was placed at the bottom of the 300 ml Teflon-lined autoclave and a hydrothermal synthesis was performed at 238 ºC for 8h with a filling percentage of 30%. The parameters for this synthesis were chosen based on the previous combination of conditions that provided the best results. After the synthesis was completed, it was noticed that a black powder was deposited on the surface of the substrate (**Figure 3.16** - in **Appendix 3** is described the substrate cleaning process) which means that nucleation points on the substrate surface were created. XRD patterns were analyzed directly by PANalytical X'Pert HighScore, which showed the expected VO_2 synthesized at these conditions: a mixture between VO_2(B) (JCPDS#81-2392) and VO_2(A) (JCPDS#42-0876) phases. The main results, which are related to the morphology tuning, can be observed in the SEM images **Figure 3.17.**

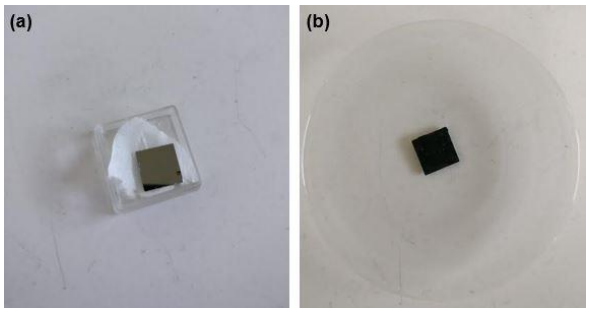

Figure 3.16. Silicon substrate orientated <100> (10 x 10 mm^2): (a) before hydrothermal synthesis; (b) after hydrothermal synthesis, with VO_2 nanostructures deposited on top, dried in the oven at 80 ºC for 15 min.

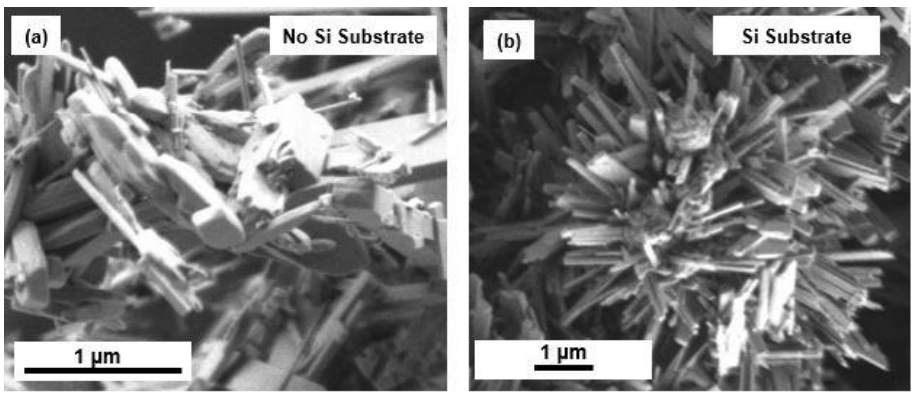

Figure 3.17. SEM images of samples synthesized at 238°C for holding 8h with a filling percentage of 30%, in order to study the influence of the presence of a Si substrate: (a) synthesis performed without Si substrate (b) synthesis performed with Si substrate.

It is interesting to observe the morphology of VO_2 nanostructures when synthesized with the presence of a Si substrate (**Figure 3.17 - b**). The obtained belts in a nanoscale and nanowires seemed to grow on the surface of the substrate according to its preferential orientation, although the nanowires are longer and do not present so many interconnections. Thus, it seems to work as a seed for VO_2 growth.

3.3. Synthesis of VO_2(M)

Since both autoclave systems undergoing the hydrothermal synthesis were limited to 250 ºC work-temperature and the required temperature to achieve the VO_2(M) phase must be higher than 260 ºC [22], other methods than hydrothermal synthesis were used in order to obtain VO_2(M). Along this chapter it is possible to analyze some alternatives ways to led to the formation of such phase.

3.3.1. Two-Step Hydrothermal Treatment

VO_2(A), with a small portion of VO_2(M) sample that was firstly synthetized through the 300 ml Teflon-lined autoclave at 238 ºC for 120h (first step), followed a second step through the same conditions for 24h. Results can be observed in **Figure 3.18**, more precisely the XRD patterns and the corresponding SEM images.

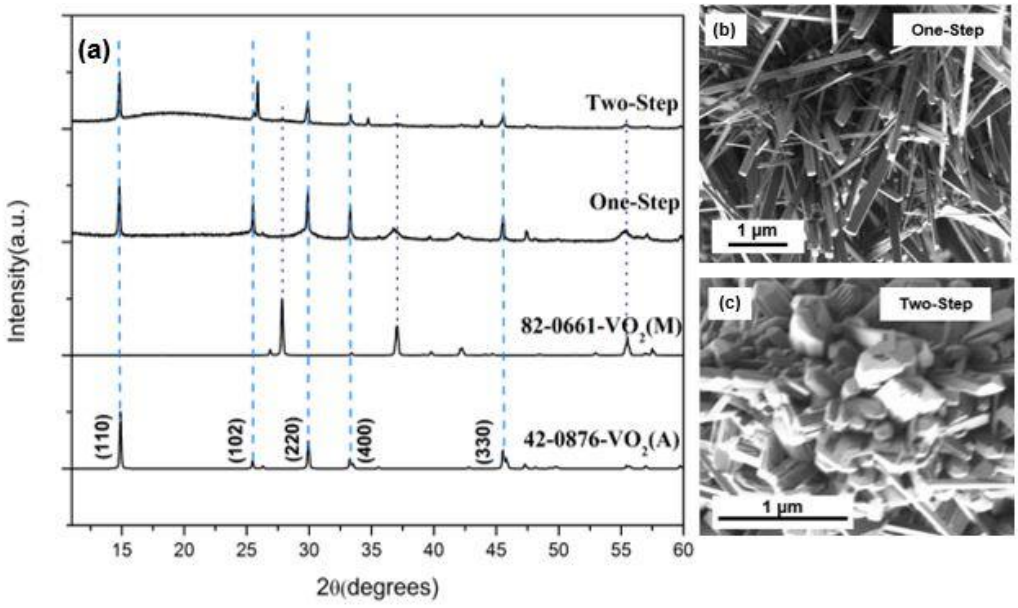

Figure 3.18. (a) XRD patterns for samples synthesized by one and a two-step hydrothermal treatment method (238°C/120h → 238°C/24h); (b-c) the corresponding SEM images.

The analysis of the one-step hydrothermal treatment is reported in **sub-section 3.1.4**, where a direct comparison between the two different filling factors is described. In these conditions, it is necessary to say that the pressure inside the cup was a little higher, arising a one-step VO_2(A) (JCPDS#42-0876) phase with some problems in the crystallinity, despite presenting a good and controlled morphology (**Figure 3.18 - b**). With the second step of hydrothermal treatment, the intensity of tetragonal VO_2(A) phase decreased in some directions, namely (220) and (330), and a small amount of VO_2(M) (JCPDS#82-0661) was formed. This result can be supported by the morphology of the particles synthesized by the two-step hydrothermal treatment (**Figure 3.18 - c**), which shows the emergence of non-defined micro-spheres that resembles VO_2(M) morphology (**Appendix 1- Figure A1.2 - d**). Part of the obtained results is coherent with Shidong Ji et. al [3], who also describe a two-step hydrothermal treatment. The authors show that a small amount of VO_2(M) appears in the sample synthesized for 24h by two-step hydrothermal treatment, despite the fact that the synthesis temperature that they used was

higher (260 ºC) than the one used in this work. In fact, it is quite probable that, to transform VO_2(A) into VO_2(M) through a two-step hydrothermal treatment at 238 ºC, it is necessary to extend the synthesis time from 24h to 72h, with controlled pressure, since the time seems to be crucial in these kind of alternative routes to produce another VO_2 polymorphs. XRD pattern of VO_2(A) phase (**Figure 3.18 - a**), which is the same as the one reported in **Figure 3.9**, presents some unknown phases that were not identified by PANalytical X'Pert HighScore. These undefined phases might be related to other intermediary VO_2 phases or to different VO_2(A) crystal structures reported in **Appendix 1**. A deeper analysis about VO_2(A) crystal structure, as the respective XRD pattern, can be found in **Appendix 6.**

3.3.2. Conventional Heating Treatment/Calcination - VO_2(B) into VO_2(M)

VO_2(B) phase obtained through 200 ml Teflon-lined autoclave (at 238 ºC for 8h with a filling percentage of 42%) was a target of a heating treatment in a tube furnace at 700 ºC for 2h [25], under argon environment, in order to be transformed to VO_2(M) rather than to V_2O_5. Results can be observed in **Figure 3.19,** which shows the XRD patterns and corresponding SEM morphology.

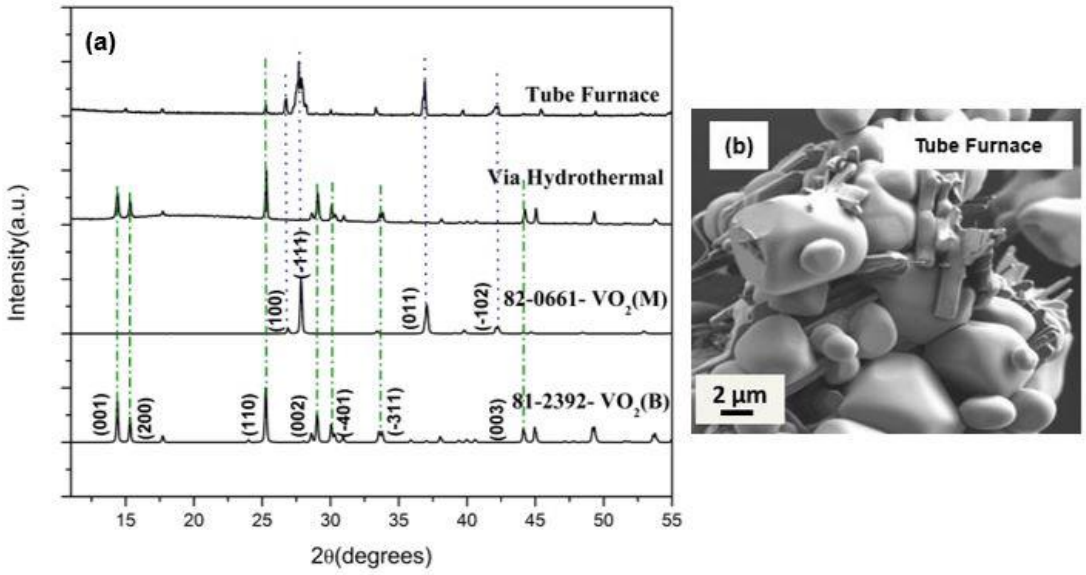

Figure 3.19. (a) XRD patterns for VO_2(B) sample synthesized by hydrothermal treatment and further heated at 700°C for 8h in a tube furnace under argon environment; (b) SEM image of VO_2(B) sample after the heating treatment.

Some diffraction peaks of the VO_2(B) sample after the heating treatment (**Figure 3.19 - a),** which can be indexed to the monoclinic VO_2(M) phase (JCPDS#82-0661) with lattice parameters of *a* = 5.743 Å, *b* = 4.157 Å, and *c* = 5.375 Å. However, the as-obtained VO_2(M) is impure, since the respective XRD pattern shows portions of VO_2(B) and undefined peaks, probably related to VO intermediate phases. SEM images (**Figure 3.19 - b**) show a microstructure composed by a mixture of micro-grains and some belt-like particles, probably of different compositions, and referring to XRD results. For the SEM images it seems that the obtained nanostructures of as synthetized samples annealed at high temperature tend to melt and form larger grains (micrometric grains). The impurity of VO_2(M) may be related to the argon atmosphere, which could not be so pure as it was supposed (<< 99.999% purity), resulting in some oxidized intermediate phases. Other reason could be related to the lock system of the furnace, which

could not be well sealed, allowing the entry of air from the surrounding environment. The presence of some VO_2(B) in the final sample may be explained by the short heating time (2h), which could not be enough to transform all VO_2(B) into VO_2(M).

By heating a sample of a previously prepared VO_2(B), it can be said that VO_2(B) can be converted into VO_2(M) by calcination under a pure argon environment at a high temperature. Through HT-XRD analysis between 100 ºC and 700 ºC and under pure argon environment, it was possible to confirm at which temperature VO_2(B) transforms into VO_2(M), although the quantity and quality of the as-obtained VO_2(B) sample was not enough to proceed with this characterization above 400ºC.

3.3.3. Raman Laser Heating – VO_2(A) into VO_2(M)

The VO_2(B) and VO_2(A) samples were characterized by Raman spectra, in order not just to have a complementary analysis about its purity but also in order to transform VO_2(A) into VO_2(M) by laser heating.

Raman bands in **Figure 3.20 - a** were characteristic of VO_2(B) [11]. The band at 140 cm^{-1} is due to lattice vibration of V_2O_5, since the partly sample of VO_2 heated for laser was oxidized into V_2O_5. The two bands at 281 cm^{-1} and 404 cm^{-1} are assigned to V_2-O and V-O flexural modes, respectively. A broad band in the range of 400-600 cm^{-1} is due to V_2-O and V_3-O bridging modes. The band at 691 cm^{-1} is attributed to V_2-O stretching vibration, while V=O stretching mode usually appeared near 1000 cm^{-1}. Raman spectrum of VO_2(B) confirms the absence of C in the as-synthesized product.

Figure 3.20 – b (i) shows all the Raman bands characteristic of VO_2(A), indicating a clear difference of VO_2(B) [11]. Still, for sample of VO_2(A) it was managed to achieve the transition phase VO_2(A) to VO_2(M) by the laser annealing.

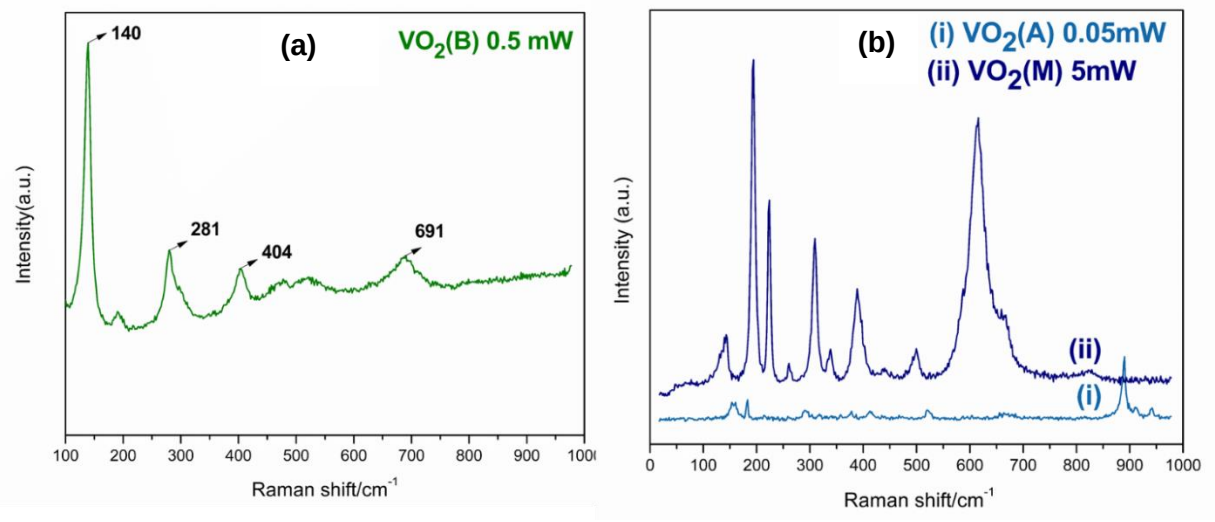

Figure 3.20. (a-c) Raman characterization of two different VO_2 samples, synthesized at different conditions: (a) Raman spectrum of the VO_2(B) sample - A200 ml, 238 ºC/8h, *f (%)* = 42%; (b) Raman spectra of the VO_2(A) sample – A200ml, 238 ºC/72h, *f (%)* = 30% in air for increasing laser powder from 0.05 mW to 5 W. Spectra have been corrected for laser power and integration time and vertically offset for clarity.

Raman spectra of this phase transition are shown in **Figure 3.20 – b (ii)**. This result is supported by the existing literature's data [47]. However, and very early in the study, the results were poorly reproduced. As **Figure 3.20 - b** shows, VO_2(A) was well transformed into VO_2(M) by increasing the laser power directly from 0.05 mW to 5 mW. The characteristics bands of as-transformed VO_2(M) can also be confirmed in reference [8]. Also, according to the literature data, and by volume, the phase of metastable tetragonal VO_2(A) transits first to rutile phase (R) at the temperature of about 350 °C and finally to monoclinic VO_2(M). In these results, the transition from tetragonal to rutile phase did not occur, which means that probably it is necessary to use an intermediate laser power to observe that intermediate transition. Some authors had write that the transition from VO_2(A) to VO_2(M) only could be achieved via hydrothermal treatment, although some researchers that studied these behaviors have concluded that is also possible to transform the tetragonal phase directly into VO_2(M) by laser annealing.

3.4. FTIR Spectroscopy Characterization

FTIR spectrum of the synthesized products was performed to confirm that the higher-quality obtained samples correspond to the VO_2(B), VO_2(A) and VO_2(A)+VO_2(B) phases, investigating the chemical boding between vanadium and oxygen ions.

Figure 3.21 shows the FTIR spectrum of VO_2(B) (hydrothermal synthesis conditions - A200 ml: T = 238 ºC, [V^{5+}] = 0.0971 mol/l, t = 8h, f *(%)* = 42%), VO_2(A) (hydrothermal synthesis conditions - A200 ml: T = 238 ºC, [V^{5+}] = 0.0971 mol/l, t = 72h, f *(%)* = 30%), and, finally, a mixture between VO_2(B) and VO_2(A) (hydrothermal synthesis conditions - A300 ml: T = 238 ºC, [V^{5+}] = 0.0971 mol/l, t = 8h, f *(%)* = 30%). The FTIR peaks obtained for each compound are characterized to the VO_2 phase and can be confirmed in references [11], [33], [48]. The main vibrational bands observed are at 606 cm^{-1}, 916 cm^{-1} and 919 cm^{-1} and in each VO_2 phase is attributed to the V-O-V octahedral bending modes and the bands at 916 cm^{-1} and 919 cm^{-1} are also attributed to the coupled vibration of V=O [33], [48]. No characteristic bands of H_2O or C, which are located at about 1624 cm^{-1} and around 2339 cm^{-1}, 2360 cm^{-1}, respectively, were detected. Authors of reference [33] explain that it is usual to find C in some VO_2 products that were synthesized by hydrothermal treatment. The presence of C is related to the surface pollution of the powder sample, which can be due to the atmosphere exposure or partial interaction with the reducing agent during the synthesis. In this case, the results indicated the absence of H_2O and C, which means that when the FTIR characterization was performed the as-obtained compounds were of high purity and did not contain absorbed water molecules on the surface. However, it is necessary to say that these compounds were characterized by FTIR after 24h of their formation, which can explain the quality observed. When some other characterizations were made to the compounds, it was observed a quality loss due to the air humidly and some impurities. FTIR results show that the used hydrothermal synthesis conditions gave rise to good quality VO_2 phases.

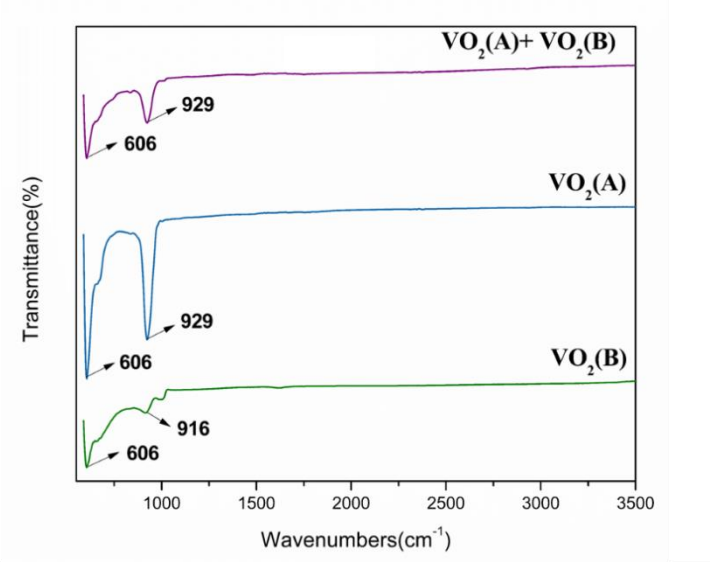

Figure 3.21. (FTIR spectrum for the samples synthesized at different conditions: VO_2(B) – A200 ml 238°C/8h, *f* (%) = 42%; VO_2(A) – A200ml, 238°C/72h, *f* (%) = 30%; VO_2(B)+VO_2(A) – A300 ml, 238°C/8h, *f* (%) = 30%.

3.5. Study the Oxidation Resistance from a Different Way

Novel and complementary analyzes that are not reported in the literature were performed in the higher-quality obtained samples to study its resistance to oxidation through DTA-DSC/HT-XRD.

The Ar environment of the DTA-DSC system was not pure from the beginning and given that this information was clear before starting the thermal behavior studies, it was decided to take the advantage of the fact that the environment was contaminated by O_2 to study the oxidation resistance of the samples instead.

Samples of pure VO_2(B) (hydrothermal synthesis conditions - A200 ml: *T* = 238 ºC, [V^{5+}] = 0.0971 mol/l, *t* = 8h, *f (%)* = 42%) and VO_2(A) (hydrothermal synthesis conditions - A200 ml: *T* = 238 ºC, [V^{5+}] = 0.0971 mol/l, *t* = 72h, *f (%)* = 30%) were used to perform DTA-DSC and identify all phase transitions. The thermal effect always accompanies the first-order phase transition and the respective results are shown in **Figure 3.22 - a and b.**

Figure 3.22 - a and b shows the heat flow curves of the as-obtained VO_2(B) and VO_2(A) samples in poor argon atmosphere. In these curves, some peaks appeared in lower temperature for both of the phases. It was not founded in the literature peaks between 60 ºC and 100 ºC. However, peaks in higher temperature side – between 300 ºC and 400ºC - reveal the oxidation process of the samples by O_2 in argon flow. The sharp endothermic peak at about 685 ºC for both phases is the melting point of V_2O_5 [25], which further confirms that the oxidative product is V_2O_5. As a result, after the characterization the final color of both powders was orange, which represents the V_2O_5 color. In order to study the formation of VO_2(B) phase between 63 ºC and 98 ºC, as well as between 300 ºC and 400ºC, the same VO_2(B) sample was characterized by HT-XRD under the air atmosphere between 25 ºC and 400 ºC. Results are shown in **Figure 3.22 - c**.

HT-XRD measurements show that VO_2(B) is stable under the air flow up to 300 ºC, and that the oxidation into V_2O_5 occurs between 300 ºC and 400ºC. The oxidation into V_2O_5 can be confirmed by the orange color of the final compound after the HT-XRD measurements. Between 25 ºC and 100 ºC no transformation occurs, which means that the peaks on heat flow curves of VO_2(B) between the same range of temperatures are not related to a phase transformation but, perhaps, to a hydrated state due to the humidity, or just a bug in the measurement, due the apparatus' conditions. Pavasupree et al. [49], who studied the stability of VO_2(B) in the air, have also observed that, around 400 ºC, VO_2(B) was oxidized into V_2O_5. Unfortunately for VO_2(A), it was not possible to conduct the same kind of characterization, more precisely due to the conditions of the sample, although based on the literature, the sample should not suffer a transformation into other VO_2 polymorph but an oxidation to V_2O_5. In terms of these oxidation results, it can be stated that the VO_2(B) and the VO_2(A) samples have good oxidation resistance properties below 302 ºC and 355ºC, respectively in argon atmosphere. The results also suggest that VO_2(A) has the best oxidation resistance, comparatively with VO_2(B), which could be beneficial for the application of VO_2(A) in the air.

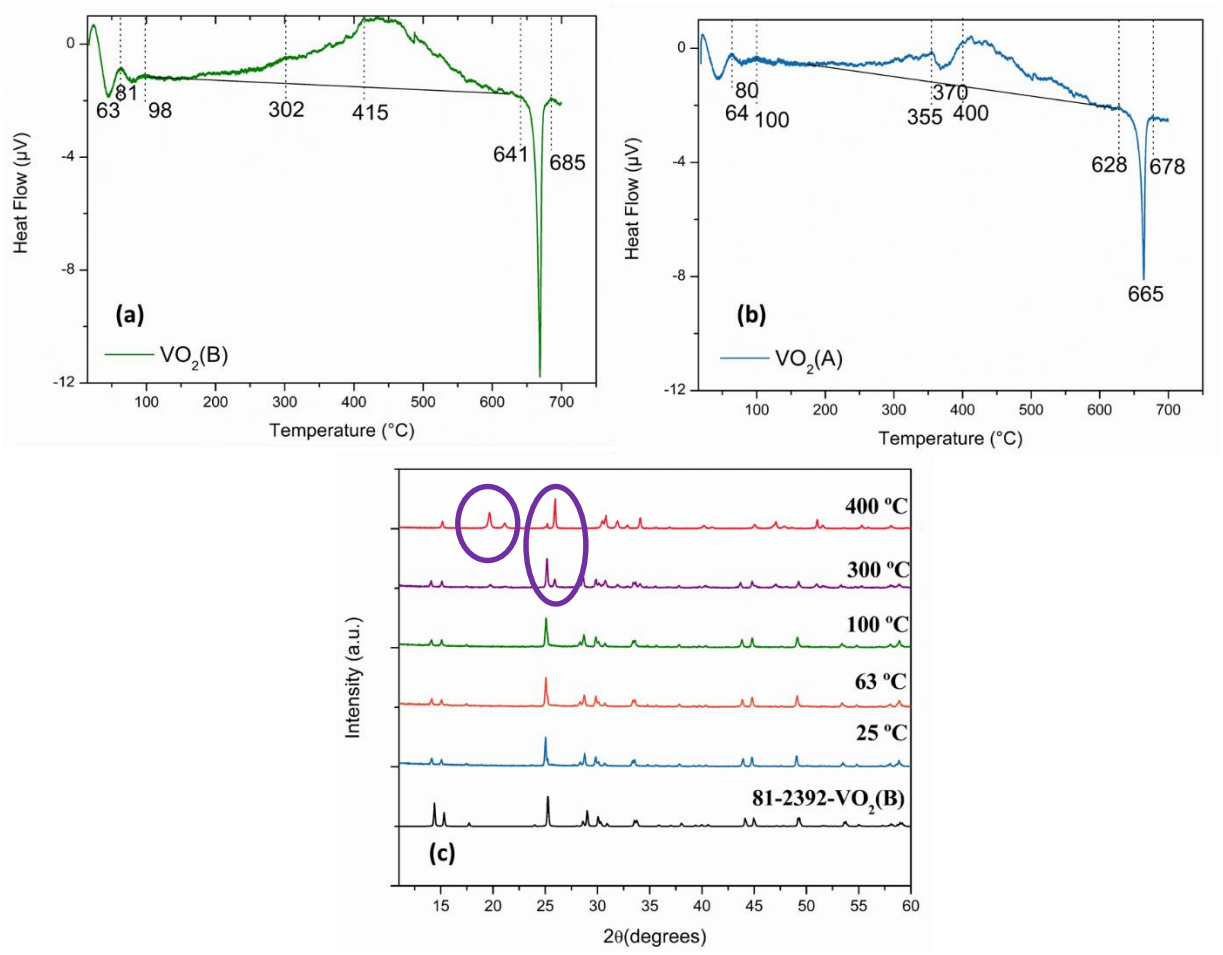

Figure 3.22. (a-b) DTA/DSC-Heat flow curves for samples synthesized at different conditions: (a) VO_2(B) - 238°C/8h, *f* (%) = 42%; (b) VO_2(A) - 238°C/72h, *f* (%) = 30%; (c) Phase transformation study of VO_2(B) by oxidation into V_2O_5 through HT-XRD from 25°C to 400°C (heating cycle under air flow). The circles highlight the transformation into V_2O_5.

Conclusion and Future Perspectives

This dissertation included the study of the synthesis of VO_2 nanostructures through the hydrothermal method. For that purpose, the influence of different synthesis parameters on the formation of VO_2 nanowires, such as synthesis temperature, V^{5+} concentration in solution, synthesis time and filling percentage, have been analyzed, while other conditions were kept constant. In general, the main strategy to prepare VO_2 under hydrothermal conditions is to reduce stable high oxidation degree of vanadium oxides, more precisely by using reductants. Besides this main study, other technical parameters were also investigated such as: the influence of the autoclave's volume, the presence of a Si crystalline seed layer; absence of Teflon liner inside the autoclave, non-stirring and the influence of extreme hydrothermal synthesis conditions. A 200 ml Teflon-lined autoclave was used to analyze the synthesis parameters above described and the hydrothermal reactions were performed from reactions of V_2O_5 with $H_2C_2O_4$ (1:(1-3) in molar ratio), except when mentioned 300 ml was also used.

The study was supported primarily by structural and morphological analyses obtained through XRD and SEM characterizations, respectively.

The study on how the temperature influences the synthesis products leads us to conclude that VO_2(B) is obtained at a synthesis temperature higher than 161 ºC but that, and even by increasing this parameter up to 238 ºC, the VO_2(B) phase remains unchanged.

The analysis about V^{5+} concentration in solution revealed that, when this parameter is too high (0.1460 mol/l) or too low (0.0486 mol/l), it is not possible to obtain the desired VO_2(A) phase and morphology. The results about its influence showed that the V^{5+} concentration in solution should be around 0.0971 mol/l in order to reach a sufficient reduction or, on the other hand, to not achieve a supersaturation state.

Synthesis time has shown that monoclinic VO_2(B) was formed at lower temperature and it changed to VO_2(A) with increasing holding time from 8h to 72h. It has been revealed a crucial parameter in order to transform VO_2(B) into tetragonal VO_2(A). However, to form VO_2(A) it is necessary to combine the synthesis time with a suitable temperature (238ºC). When the synthesis time increased from 72h to 120h it was noticeable that the intensity of some VO_2(A) directions started decreasing, which could mean a formation of a new VO_2 phase. Unfortunately, synthesis time analyses did not take into consideration the 120h, since it was also intended to grow the desired phases within the short time possible. System pressure, that became high with the increase in filling percentage or in temperature, was considered to be a critical factor, which decisively determines the VO_2(A) transformation into other VO_2 polymorphs. When the pressure was too high, due to the extreme conditions used, anomalous structures with some undefined phases and a trace of VO_2(M) have been formed, meaning that the phase transformation from VO_2(A) is pressure sensitive. Based on the experiments carried through the 200 ml and 300 ml Teflon-lined autoclaves, it was noticed that the formation of desired VO_2 nanostructures is very dependent on the chamber used for the reaction, which means that the control of the synthesis parameters is very dependent on the volume and the material of the container. Additional experiments have shown that the Teflon vessel has a great influence on the formation of VO_2 nanostructures, since it allows final products with homogeneous morphology, due to the fact that it avoids nucleation points on the steel walls.

Two-step hydrothermal treatment performed for holding 24h was not effective to transform a mixture between VO_2(A) and a small portion of VO_2(M) in a pure VO_2(M) phase, perhaps due to the high pressure during the synthesis.

For the morphology study purpose, while the role of stirring has no influence on the VO_2 morphology, the addition of a Si substrate <100> at the bottom of the autoclave promotes the growth of VO_2 nanoparticles in particular directions. No other pure phases than VO_2(B) or VO_2(A) through hydrothermal synthesis, in this dissertation, were obtained, only a few amount of VO_2(M) phase appeared when the pressure inside the cup increased. Other routes than hydrothermal synthesis were performed to transform the two-obtained VO_2 phases into VO_2(M): VO_2(B) was successfully transformed into VO_2(M) phase by calcination in a tube furnace at 700 ºC for 2h under argon environment, VO_2(A) was also directly transformed into VO_2(M) by laser annealing with a power of 5 mW. FTIR and Raman measurement provided the obvious evidence of VO_2(B) and VO_2(A). DSC and HT-XRD analyzes were very useful to study the oxidation properties and thermal effect of phase transitions on the as-obtained VO_2(B) and VO_2(A) samples, showing that those samples had good thermal stability and oxidation resistance below 302 ºC and 355 ºC, respectively, in impure argon atmosphere. VO_2(A) nanostructures had the best oxidation resistance, which can be beneficial for the application of VO_2(A) in the air. In addition, this dissertation refers to other two VO_2(A) space groups, despite the fact that it does not proceed to a deeper analysis.

It was believed that the present dissertation provides effective routes to control the desired VO_2 morphs and that it also helps to understand the basic properties of VO_2, especially for monoclinic VO_2(B) and tetragonal VO_2(A). It is important to refer that the versatility of hydrothermal synthesis can be extended to the preparation of other transition metal oxides.

In spite of these achievements, much remaining studies are necessary. It would also be interesting to study the influence of other conditions on the formation of VO_2 nanostructures, mainly the influence of the pH by adding H_2SO_4 (sulfuric acid); the influence of doping during the hydrothermal synthesis with W or F atoms, in order to study their impact on the structural and electronic VO_2 phase diagrams; and the influence of 2-phenylethylamine and 4-phenylbutylamine as structure-directing templates.

Since the temperature also represents a very important factor on the formation of VO_2 nanostructures, it could also be interesting to perform hydrothermal syntheses through a system that allows the increasing of temperature up to 270 ºC. Perhaps with this adjustment, the sequential transitions VO_2(B)→VO_2(A)→VO_2(R)→VO_2(M) may occur.

Unfortunately, and for technical reasons, it was not possible to perform the analysis of the as-obtained samples by TEM. Then, and for future work, it may be very useful to study the final products.

So far, it is known that VO_2(A) can be transformed into VO_2(M), although the reverse was not verified. This fact, and the two different VO_2(A) space groups that were discovered recently, can be target of study. This study has many opportunities for optimization, with the major final goal to produce crystalline VO_2 polymorphs with desirable morphology, through hydrothermal synthesis, for further applications, in particular MOTTFETS.

References

[1] G. S. Zakharova, N. V. Podval'naya, and M. V. Kuznetsov, "XPS study of nanorods of doped vanadium oxide $MxV_2O_5nH_2O$ (M = Na, K, Rb, Cs)," *Russ. J. Inorg. Chem.*, vol. 56, no. 2, pp. 267–272, 2011.

[2] Y. Zhang, C. Huang, and C. Meng, "one-pot hydrothermal process and their effect on thermal decomposition of ammonium perchlorate," vol. 5, no. 2, pp. 105–112, 2015.

[3] S. D. Ji, F. Zhang, and P. Jin, "Formation mechanisms and crystallographic characteristics of metastable VO_2(A) nanofiber hydrothermally synthesised in V_2O_5-$H_2C_2O_4$-H_2O system," *J. Phys. Chem. Solids*, vol. 73, no. 6, pp. 762–769, 2012.

[4] H. Y. Li, X. Qiu, M. Dong, X. Li, Y. Zhang, and B. Xie, "Tuned hydrothermal synthesis of vanadium dioxide nanotubes," *Ceram. Int.*, pp. 1–7, 2015.

[5] M. Li, F. Y. Kong, Y. X. Zhang, and G. H. Li, "Hydrothermal synthesis of VO_2(B) nanorings with inorganic V_2O_5 sol," *Crystengcomm*, vol. 13, no. 7, pp. 2204–2207, 2011.

[6] J. Livage, "Hydrothermal Synthesis of Nanostructured Vanadium Oxides," *Materials (Basel).*, vol. 3, no. 8, pp. 4175–4195, 2010.

[7] R. S. Devan, R. A. Patil, J. H. Lin, and Y. R. Ma, "One-dimensional metal-oxide nanostructures: Recent developments in synthesis, characterization, and applications," *Adv. Funct. Mater.*, vol. 22, no. 16, pp. 3326–3370, 2012.

[8] P. Vilanova-Martínez, J. Hernández-Velasco, A. R. Landa-Cánovas, and F. Agulló-Rueda, "Laser heating induced phase changes of VO_2 crystals in air monitored by Raman spectroscopy," *J. Alloys Compd.*, vol. 661, pp. 122–125, 2016.

[9] H. Jerominek, "Vanadium oxide films for optical switching and detection," *Opt. Eng.*, vol. 32, no. 9, p. 2092, 1993.

[10] Y. Zhang, J. Zhang, X. Zhang, S. Mo, W. Wu, F. Niu, Y. Zhong, X. Liu, C. Huang, and X. Liu, "Direct preparation and formation mechanism of belt-like doped VO_2(M) with rectangular cross sections by one-step hydrothermal route and their phase transition and optical switching properties," *J. Alloys Compd.*, vol. 570, pp. 104–113, 2013.

[11] H. F. Xu, Y. Liu, N. Wei, and S. W. Jin, "From VO_2(B) to VO_2(A) nanorods: Hydrothermal synthesis, evolution and optical properties in $V_2O_5H_2C_2O_4H_2O$ system," *Optik (Stuttg).*, vol. 125, no. 20, pp. 6078–6081, 2014.

[12] T. V. O. M, S. R. Popuri, M. Miclau, A. Artemenko, C. Labrugere, and A. Villesuzanne, "Rapid Hydrothermal Synthesis of VO_2(B) and Its Conversion to Thermochromic VO_2 (M1)," *Inorg. Chem.*, vol. 2, pp. 4780–4785, 2013.

[13] Y. Zhang, X. Zhang, Y. Huang, C. Huang, F. Niu, C. Meng, and X. Tan, "One-step hydrothermal conversion of VO_2(B) into W-doped VO_2(M) and its phase transition and optical switching properties," *Solid State Commun.*, vol. 180, pp. 24–27, 2014.

[14] S. Ji, F. Zhang, and P. Jin, "Selective formation of VO_2(A) or VO_2(R) polymorph by controlling the hydrothermal pressure," *J. Solid State Chem.*, vol. 184, no. 8, pp. 2285–2292, 2011.

[15] L. Dai, C. Cao, Y. Gao, and H. Luo, "Synthesis and phase transition behavior of undoped VO_2 with a strong nano-size effect," *Sol. Energy Mater. Sol. Cells*, vol. 95, no. 2, pp. 712–715, 2011.

[16] AM. Makarevich, I. I. Sadykov, D. I. Sharovarov, V. A. Amelichev, A. A. Adamenkov, D. M. Tsymbarenko, A. V. Plokhih, M. N. Esaulkov, P. M. Solyankin, and A. R. Kaul, "Chemical synthesis of high quality epitaxial vanadium dioxide films with sharp electrical and optical switch properties," *J. Mater. Chem. C*, vol. 3, no. 35, pp. 9197–9205, 2015.

[17] C. Ko, Y. Zhou, and S. Ramanathan, "Probing compositional disorder in vanadium oxide thin films grown on atomic layer deposited hafnia on silicon by capacitance spectroscopy," *J. Vac. Sci. Technol. A Vacuum, Surfaces, Film.*, vol. 30, no. 1, p. 11501, 2012.

[18] Z. Hiroi, "Structural instability of the rutile compounds and its relevance to the metal-insulator transition of VO_2," *Prog. Solid State Chem.*, vol. 43, no. 1–2, pp. 47–69, 2015.

[19] Z. Yang, C. Ko, and S. Ramanathan, "Oxide Electronics Utilizing Ultrafast Metal-Insulator Transitions," *Annu. Rev. Mater. Res.*, vol. 41, no. 1, pp. 337–367, 2011.

[20] J. P. Pouget and H. Launois, "Metal-Insulator Phase Transition in VO_2," *Le J. Phys. Colloq.*, vol. 37, no. C4, pp. C4-49-C4-57, 1976.

[21] Z. Jin, I. Hwang, C. Park, J. Son, and S. Han, "Synthesis and temperature-dependent local structural and electrical properties of VO_2 films," *Curr. Appl. Phys.*, vol. 16, no. 2, pp. 183–190, 2016.

[22] S. Ji, Y. Zhao, F. Zhang, and P. Jin, "Direct formation of single crystal VO_2(R) nanorods by one-step hydrothermal treatment," *J. Cryst. Growth*, vol. 312, no. 2, pp. 282–286, 2010.

[23] M. Dragoman, A. Cismaru, H. Hartnagel, and R. Plana, "Reversible metal-semiconductor transitions for microwave switching applications," *Appl. Phys. Lett.*, vol. 88, no. 7, pp. 2004–2007, 2006.

[24] S. D. Ha, Y. Zhou, C. J. Fisher, S. Ramanathan, and J. P. Treadway, "Electrical switching dynamics and broadband microwave characteristics of VO_2 radio frequency devices," *J. Appl. Phys.*, vol. 113, no. 18, 2013.

[25] Y. Zhang, "VO_2(B) conversion to VO_2(A) and VO_2(M) and their oxidation resistance and optical switching properties," *Mater. Sci.*, vol. 34, no. 1, pp. 169–176, 2016.

[26] L. Bjaalie, B. Himmetoglu, L. Weston, A. Janotti, and C. G. Van De Walle, "Oxide interfaces for novel electronic applications," *New J. Phys.*, vol. 16, 2014.

[27] T.-J. K. Liu, "CMOS and Beyond- Logic Switches for Terascale Integrated Circuits," California: Press, Cambridge University, 2015, pp. 209–211.

[28] S. Hormoz and S. Ramanathan, "Limits on vanadium oxide Mott metal-insulator transition field-effect transistors," *Solid. State. Electron.*, vol. 54, no. 6, pp. 654–659, 2010.

[29] J. Yoon, H. Kim, X. Chen, N. Tamura, B. S. Mun, C. Park, and H. Ju, "Controlling the temperature and speed of the phase transition of VO_2 microcrystals," *ACS Appl. Mater. Interfaces*, p. acsami.5b11144, 2015.

[30] O. M. Osmolovskaya, I. V Murin, V. M. Smirnov, and M. G. Osmolovsky, "Synthesis of Vanadium Dioxide Thin Films and Nanopowders : a Brief Review," *Rev. Adv. Mater. Sci.*, vol. 36, pp. 70–74, 2014.

[31] E. Strelcov, A. Tselev, I. Ivanov, J. D. Budai, J. Zhang, J. Z. Tischler, I. Kravchenko, S. V. Kalinin, and A. Kolmakov, "Doping-based stabilization of the M2 phase in free-standing VO2 nanostructures at room temperature," *Nano Lett.*, vol. 12, no. 12, pp. 6198–6205, 2012.

[32] H. Hayashi and Y. Hakuta, "Hydrothermal Synthesis of Metal Oxide Nanoparticles in Supercritical Water," *Materials (Basel).*, vol. 3, no. 7, pp. 3794–3817, 2010.

[33] S. R. Popuri, M. Miclau, A. Artemenko, C. Labrugere, A. Villesuzanne, and M. Pollet, "Rapid hydrothermal synthesis of VO_2(B) and its conversion to thermochromic VO_2(M1)," *Inorg. Chem.*, vol. 52, no. 9, pp. 4780–4785, 2013.

[34] O. R. Bingöl and C. Durucan, "Hydrothermal Synthesis of Hydroxyapatite from Calcium Sulfate Hemihydrate," *Am. J. Biomed. Sci.*, vol. 4, no. 1, pp. 50–59, 2012.

[35] M. Vijayakumar, "Development of rare earth based lithium silicates and nanocomposite polymer solid electrolytes for lithium battery applications," Pondicherry University, 2012.

[36] D. V Tawde, "Structural and optical studies of cerium doped lead tungstate nano phosphor," Maharaja Sayajirao University of Baroda, 2013.

[37] S. Rao Popuri, A. Artemenko, C. Labrugere, M. Miclau, A. Villesuzanne, and M. Pollet, "VO_2(A): Reinvestigation of crystal structure, phase transition and crystal growth mechanisms," *J. Solid State Chem.*, vol. 213, pp. 79–86, 2014.

[38] S. Ji, Y. Zhao, F. Zhang, and P. Jin, "Synthesis and phase transition behavior of W-doped VO_2(A) nanorods," *J. Ceram. Soc. Japan*, vol. 2, pp. 867–871, 2010.

[39] S. Ji, F. Zhang, and P. Jin, "Phase transition of single crystal VO_2(R) nanorods in solution revealed by reversible change in surface charge state and structure," *Mater. Lett.*, vol. 65, no. 4, pp. 708–711, 2011.

[40] Y. Zhang, M. Fan, X. Liu, G. Xie, H. Li, and C. Huang, "Synthesis of VO_2(A) nanobelts by the transformation of VO_2(B) under the hydrothermal treatment and its optical switching properties," *Solid State Commun.*, vol. 152, no. 4, pp. 253–256, 2012.

[41] M. Zaghrioui, J. Sakai, N. H. Azhan, K. Su, and K. Okimura, "Polarized Raman scattering of large crystalline domains in VO_2 films on sapphire," *Vib. Spectrosc.*, vol. 80, pp. 79–85, 2015.

[42] D. B. Macnaughton, "Generalization of Eight Methods for Determining R in the Ideal Gas Law."

[43] S. Wang, Z. Lu, D. Wang, C. Li, and C. Chen, "Porous monodisperse V 2 O 5 microspheres as cathode materials for lithium-ion batteries (a) (b) (c) (d) (e) (f) (a) (b)," vol. 6, no. c, pp. 3–5, 2011.

[44] J. Galy, "A Proposal for VO_2(B) -> VO_2(B) Phase Transition : A Simple Crystallographic Slip," *J. Solid*, vol. 148, pp. 224–228, 1999.

[45] S. Ni, H. Zeng, and X. Yang, "Fabrication of VO_2(B) nanobelts and their application in lithium ion batteries," *J. Nanomater.*, vol. 2011, pp. 1–5, 2011.

[46] W. Yu, S. Li, and C. Huang, "Phase evolution and crystal growth of VO_2 nanostructures under hydrothermal reactions," *RSC Adv.*, vol. 6, no. 9, pp. 7113–7120, 2016.

[47] S. Zhang, I. S. Kim, and L. J. Lauhon, “Stoichiometry engineering of monoclinic to rutile phase transition in suspended single crystalline vanadium dioxide nanobeams,” *Nano Lett.*, vol. 11, no. 4, pp. 1443–1447, 2011.

[48] F. Sediri and N. Gharbi, “Nanorod B phase VO2 obtained by using benzylamine as a reducing agent,” *Mater. Sci. Eng. B Solid-State Mater. Adv. Technol.*, vol. 139, no. 1, pp. 114–117, 2007.

[49] S. Pavasupree, Y. Suzuki, A. Kitiyanan, S. Pivsa-Art, and S. Yoshikawa, “Synthesis and characterization of vanadium oxides nanorods,” *J. Solid State Chem.*, vol. 178, no. 6, pp. 2152–2158, 2005.

[50] F. Theobald, “Hydrothermal Study of VO_2-$VO_{2.5}$-H_2O System,” *J. Less-Common Met.*, vol. 53, pp. 55–71, 1977.

[51] Y. Oka, T. Ohtani, N. Yamamoto, and T. Takada, “Phase Transition and electrical properties of VO_2(A),” *J. Ceram. Soc. Jpn*, vol. 97, no. 10, pp. 1134–1137, 1989.

[52] J. H. Son, J. Wei, D. Cobden, G. Cao, and Y. Xia, “Hydrothermal synthesis of monoclinic VO_2 micro- and nanocrystals in one step and their use in fabricating inverse opals,” *Chem. Mater.*, vol. 22, no. 10, pp. 3043–3050, 2010.

A1 Appendix 1

Crystallography Data and Morphology Type of VO_2 Polymorphs

Table A1.1. The crystallography data of some important types of VO_2 polymorph [26].

Phase	Tc *[ºC]	Cs*	Sg*	a [Å]	b [Å]	c [Å]	β [Å]
VO_2(B)	-	Monoclinic	C2/m	12.03	3.69	6.42	106.60
VO_2(M)	68	Monoclinic	$P2_1/c$	5.74	4.16	5.38	122.60
VO_2(R)	68	Tetragonal	$P4_2/mnm$	4.530	4.530	2.869	-
VO_2(A)	-	Tetragonal	$P4_2/nmc$	8.44	8.44	7.67	
$VO_2(A_{LTP})$	162	Tetragonal	P4/ncc	8.44	8.44	7.67	-
$VO_2(A_{HTP})$	162	Tetragonal	I4/m	8.48	8.48	3.82	-

*Tc: Critical temperature for phase transition; Cs: Crystal system; Sg: Space Group

Observations about VO_2(A) phases: The synthesis of VO_2(A) polymorph was first reported in 1977 by Theobald [50], where was shown that VO_2(A) crystallizes in tetragonal symmetry with lattice parameters *a* = 11.90 Å and *c* = 7.68 Å, but the space group was unknown at that time. Few years later, in 1989, Oka et al. [51] prepared VO_2(A) particles by hydrothermal process and studied its phase transition and some electrical properties. The authors observed a discontinuity in the evolution of the lattice at 435 K, which was associated with a structural phase transition. Oka et al., followed by Yao et al., solved the crystal structure of hydrothermally synthesized polycrystalline samples of VO_2(A), assigning the space group $P4_2/nmc$ with lattice parameters *a* = 8.433 Å and *c* = 7.678 Å. Although, Oka et al. reinvestigated the crystal structure of VO_2(A) by single crystal diffractometry and proposed that, at 298 K, VO_2(A), low temperature phase (A_{LTP}) adopts the P4/ncc space group with *a* = b 8.44 Å and *c*= 7.67 Å. On the other hand, at 473 K, VO_2(A) high temperature phase (A_{HTP}) adopts the I4/m space group with *a* = 8.48 Å and c= 3.82 Å.

An extensive review about the VO_2(A) structural transition can be found in reference [37], where the authors describe the discrepancies about the VO_2(A) space group, reinvestigating its phase transition under hydrothermal conditions.

Simulation of VO_2(A) phases (LTP and HPT): As the two mentioned VO_2(A) space groups (I4/m and P4/ncc) are not present in the JCPDS data base, it was decided to perform a simulation of their XRD patterns through FullProf software in order to observe the main differences between the XRD peaks of 42-0876 VO_2(A) (P42/nmc space group) and VO_2(A) (P4/ncc and I4/m space groups) (**Figure A1.1**).

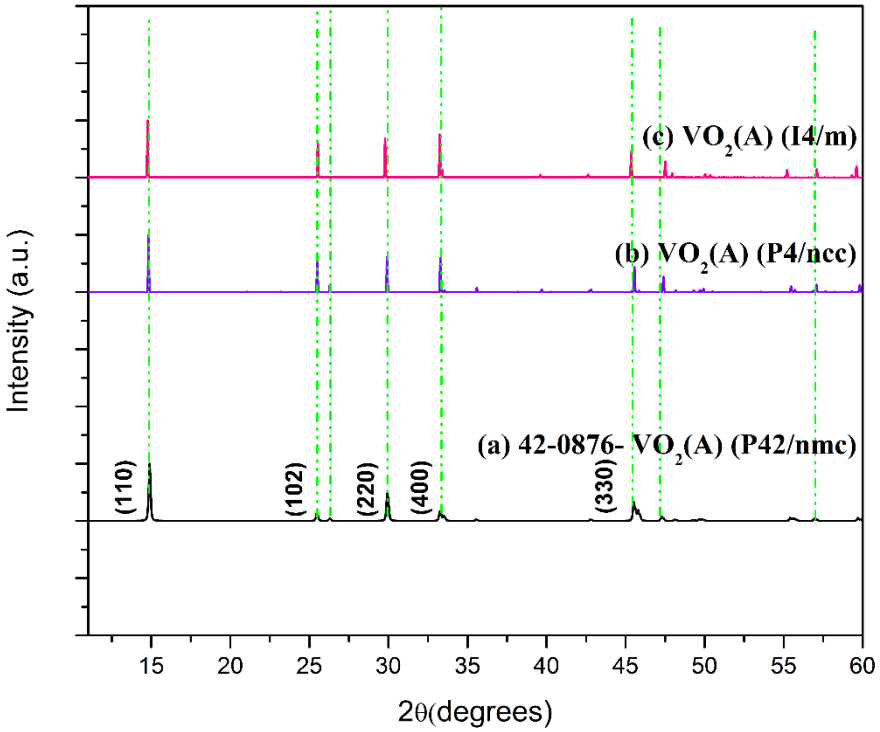

Figure A1.1. XRD patterns of VO_2(A) phases (a): JCPDS 42-0876 VO_2(A) (P42/nmc space group), (b) simulated VO_2(A) (P4/ncc) space group); (c) simulated VO_2(A) (I4/m space group).

Observations: As stated above, **Figure A1.1** shows the original VO_2(A) phase presented in the JCPDS data base and the respective VO_2(A) low temperature and high temperature phase simulations. By observing their respective peaks, no significant difference is presented, just some few non-intense peaks between $2\theta = 35^0$ and 45^0 . Since these new VO_2(A) patterns are based on simulations, it was decided to keep the original JCPDS VO_2(A) for analysis results section. The aim of this work is not related to a deep research about VO_2(A) phase and its respective space groups. Thus, this kind of study can be continued in the future. Although, it was decided to compare an obtained VO_2(A) sample with these two new space groups, since the patterns showed some undefined phases. Such analysis can be consulted in **Appendix 6.**

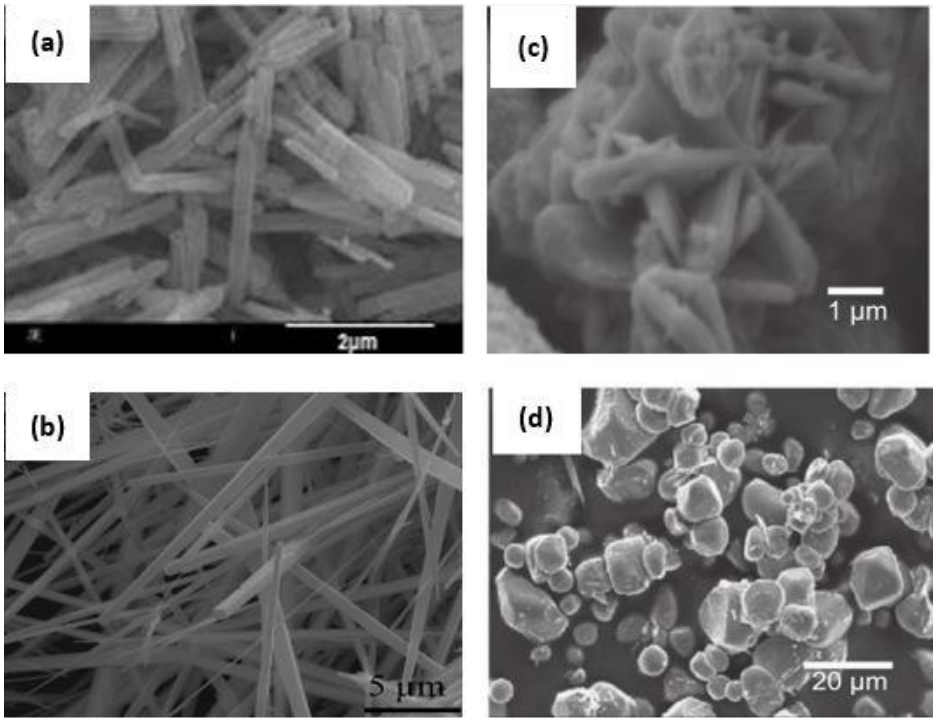

Figure A1.2. Morphology of different VO_2 polymorph samples: (a) VO_2(B) Belt-like morphology; (b) VO_2(A) Wire-like morphology; (c) VO_2(M) snow flake aggregation; (d) VO_2(M) Micro-Spheres [14], [37], [52].

Observations: VO_2(A) phase presents at least two different types of morphology, depending on the hydrothermal synthesis conditions used to carry the treatment. VO_2(A), apart from providing micro and nanowires, also provides micro e nanorods with and without a rectangular section, as it is possible to confirm in **Figure A1.3**.

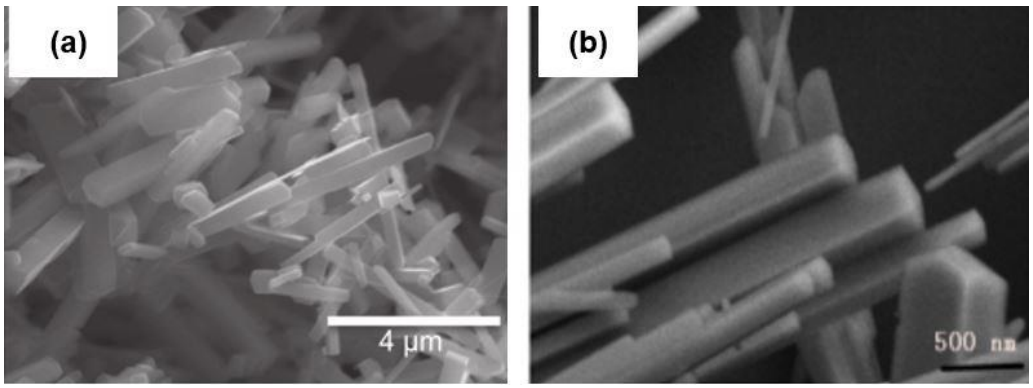

Figure A1.3. Morphology of the some VO_2(A) phase final product depending on the experimental hydrothermal synthesis conditions: (a) VO_2(A) microrods; (b) VO_2(A) microrods with rectangular section [11], [37].

A2 Appendix 2

Autoclave's Specifications

Table A2.1. Specifications from the Autoclave Maxitech France composed of a stainless steel body of 200 ml.

Autoclave Maxitech France-Stainless steel body 200 ml in capacity	
Supplier	*Autoclave France*
Type	Opening Fast Reactor
Year	2009
Serial number	12-0888-1
Maximum operating pressure	234 bar
Maximum operating temperature	250 ºC

Table A2.2. Specifications from the Autoclave Maxitech France composed of a stainless steel body of 300 ml.

Autoclave Maxitech France 300 ml- Stainless steel body of 300 ml in capacity	
Supplier	*Autoclave France*
Type	Opening Fast Reactor
Year	2009
Serial number	12-0888-2
Maximum operating pressure	234 bar
Maximum operating temperature	250 ºC

Figure A2.1. Autoclave Maxitech France components: (a) steel bodies (200 ml and 300 ml in capacity) with respective Teflon liners inside; (b) heating oven with support; (c) temperature safety regulator (Invensys Eurotherm 3216); (d) process temperature regulator (Invensys Eurotherm 3208).

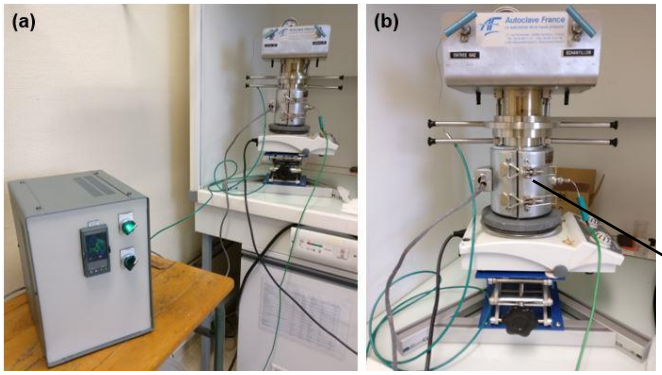

Figure A2.2. Setup for hydrothermal synthesis: (a) oven surrounding the steel body and thermocouple connected to the process temperature and temperature safety regulators, respectively. Both the steel body and the oven were placed on a hotplate stirrer; (b) Magnified setup image that's shows clearly the Autoclave sealing system.

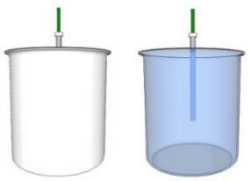

Figure A2.3. Sketch drawing of the thermocouple position inside the Teflon liner.

A3 Appendix 3

Si substrate <100> Cleaning Process

Substrate: Silicon substrate (10 x 10 mm^2) in wafers <100>- International Wafer Service
Conditions and steps:
1) Immersing in Acetone for 2 min.
2) Washing with deionized water.
3) Immersing in Isopropanol for 2 min.
4) Washing with deionized water.

A4 Appendix 4

Hydrothermal Synthesis Conditions of Additional Experiments

Table A4.1. Experimental extreme conditions applied to the hydrothermal synthesis to study their effect on VO_2 nanostructures, regarding different filling percentages. Experiments carried out through a steel body of 300 ml.

Hydrothermal Synthesis Conditions Taken to the Extreme ***300 ml*** *Steel body with a Teflon liner of* ***233 ml***						
Series Number	**Parameters**					
	Autoclave's Volume (ml)	**T(ºC)**	**$[V^{5+}]$ (mol/l)**	**t (h)**	**f (%)**	
6	300	238	0.0971	120	30	60

Table A4.2. Experimental conditions applied to the hydrothermal synthesis to study the effect of the non-presence of the Teflon liner on VO_2 nanostructures. Experiments carried out through a steel body of 200 ml with a Teflon liner of 144 ml.

Hydrothermal Synthesis Conditions: Effect of Teflon liner ***200 Steel*** *body ml with a Teflon liner of* ***144 ml***						
Series Number	**Parameters**					
	Teflon liner		**T(ºC)**	**$[V^{5+}]$ (mol/l)**	**t (h)**	**f (%)**
7	yes	no	238	0.0971	72	30

Table A4.3. Experimental conditions applied to the hydrothermal synthesis to study the effect of the non-stirring of the Teflon liner on VO_2 nanostructures. Experiments carried out through a steel body of 300 ml with a Teflon liner of 233ml.

Hydrothermal Synthesis Conditions: Effect of Non-Stirring ***300 ml*** *Steel body with a Teflon liner of* ***233 ml***						
Series Number	**Parameters**					
	Stirring		**T(ºC)**	**$[V^{5+}]$ (mol/l)**	**t (h)**	**f (%)**
8	yes	no	238	0.0971	8	30

A5 Appendix 5

Experimental Details and Respective XRD Results of all Hydrothermal Syntheses Performed

Table A5.1. Experimental details of the all hydrothermal synthesis performed along the present work as well as the respective XRD results.

All of Hydrothermal Synthesis Conditions Performed and Respective Results						
Sample	**Tl (y/n)**	**[V^{5+}] (mol/l)**	**f (%)**	**t (h)**	**T (ºC)**	**XRD Results**
1	Y	0.0971	42%-60ml	8	226	VO_2(B)
2	Y	0.0971	42%-60ml	4	226	VO_2(B)
3	Y	0.0971	42%-60ml	8	212	VO_2(B)
4	Y	0.0971	42%-60ml	8	191	VO_2(B)
5	Y	0.0971	42%-60ml	8	238	VO_2(B)
6	Y	0.0971	42%-60ml	8	185	VO_2(B)
7	Y	0.0971	42%-60ml	8	161	$V_3O_7(H_2O)$ + $V_2O_5.0.5H_2O$
8	Y	0.0971	42%-60ml	24	199	VO_2(B)
9	Y	0.0971	30%-42ml	8	238	VO_2(B)
10	Y	0.0971	42%-60ml	8	199	VO_2(B)
11	N	0.0971	30%-60ml	8	257	VO_2(B)
12	Y	0.0971	30%-42ml	8	205	VO_2(B)
13	N	0.0971	30%-60ml	72	238	VO_2(A) + VO_2(B)
14	N	0.0486	30%-60ml	8	238	VO_2(B)
15	Y	0.0486	30%-42ml	8	238	$V_3O_7(H_2O)$ + VO_2(B)
16	Y	0.0971	30%-42ml	72	238	VO_2(A)
17	Y	0.1460	30%-42ml	8	238	VO_2(B) + VO_2(A)
18	Y	0.0971	30%-42ml	24	220	Undefined Results
19	Y	0.0971	30%-42ml	72	228	Undefined Results
20	Y	0.0971	30%-42ml	72	234	Undefined Results
21	Y	0.0971	30%-70ml	8	238	VO_2(A) + VO_2(B)
22	Y	0.0971	30%-42ml	120	238	VO_2(A)
23	Y	0.1460	30%-70ml	120	238	VO_2(A) + VO_2 derivatives
24	Y	Powder 25	30%-70ml	24	238	VO_2(A) + VO_2 derivatives
25	Y	0.0971	30%-70ml	120	238	System has stopped
26	Y	0.0971	30%-70ml	240	238	Undefined Results
27	Y	0.0971	60%-140ml	120	238	Undefined Results
28	Y	0.0971	30%-70ml	8	238	VO_2(A) + VO_2(B)- **non-stirring**
29	Y	0.0971	30%-70ml	8	238	VO_2(A)+ VO_2(B)- **Si substrate**
30	Y	0.0971	30%-70ml	72	238	VO_2(A) not crystalline
31	Y	0.0971	30%-70ml	120	238	VO_2(A) not crystalline

A6 Appendix 6

Deeper Analysis about VO_2(A) Phase Space Groups

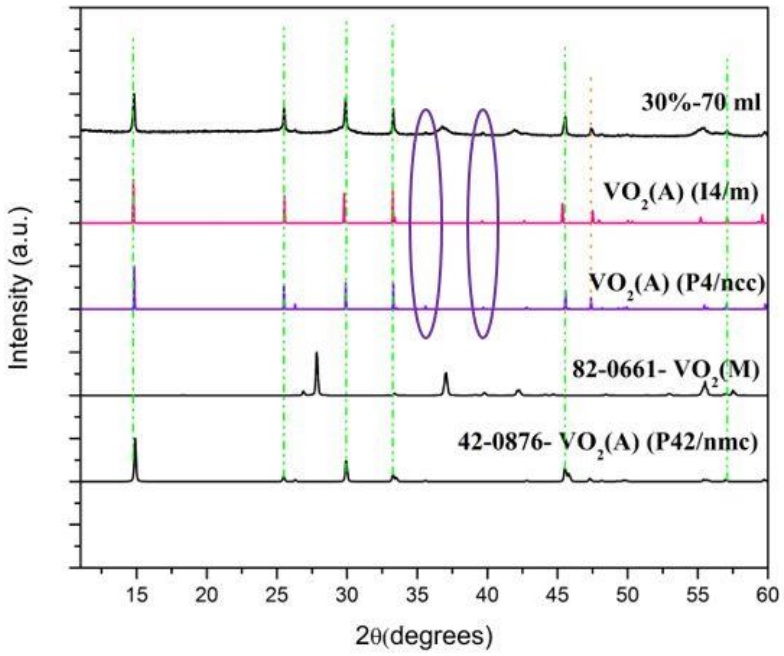

Figure A6.1. XRD pattern of VO_2(A) phase sample synthesized through the 300 ml Teflon-lined autoclave, at 238 ºC for 120h with a filling percentages of 30%, compared with the simulated VO_2(A) phases (P4/ncc and I4/m space groups), in order to verify any peaks correspondence. The circles highlight the undefined peaks of the VO_2(A) synthesized sample and its correspondence with the ones related to the simulated phases.

Observations: **Figure A6.1** shows a deeper analysis of the VO_2(A) phase obtained at 238 ºC for 120h with a filling percentages of 30% through the 300 ml Teflon-lined autoclave. In the previous analysis detailed in **Results and Discussion section**, it was found out that some peaks of this as-obtained VO_2(A) sample were unknown. A reason had been given for the appearance of this peaks: it could be related to intermediate VO derivatives that were formed during the synthesis. However, to ensure this results it was decided to perform a simulation of the new VO_2(A) space groups: P4/ncc and I4/m, corresponding to high temperature A phase and low temperature A phase, respectively, in order to observe some correspondence. Actually, by observing the circles in **Figure A6.1** it is noticed that some of the first unknown peaks seem to correspond to the one of the new VO_2(A) space groups, perhaps to the space group P4/ncc, since the synthesis was performed at 238ºC (>> 162 ºC). These results give the impression that the new VO_2(A) space group was formed during the hydrothermal synthesis. However, these new patterns are just based on a simulation, so it is not possible to have absolutely sure about the occurrence of a VO_2(A) transformation. Therefore, it was not possible to conclude what was the source of those undefined peaks.

Further studies related to intrinsic electrical properties of VO_2(A) are in progress to clarify the exact nature of the electronic transition.